

Chemical compositions and kinematics of the Hercules stream

P. Ramya,^{1*} Bacham E. Reddy¹, David L. Lambert² and M. M. Musthafa³

¹*Indian Institute of Astrophysics, Bengaluru, India-560034*

²*The W.J. McDonald Observatory & Department of Astronomy, University of Texas at Austin, Austin, TX 78712, USA*

³*University of Calicut, Malappuram, India-673635*

Accepted Received ; in original form

ABSTRACT

An abundance analysis is reported of 58 K giants identified by Famaey et al. (2005) as highly probable members of the Hercules stream selected from stars north of the celestial equator in the *Hipparcos* catalogue. The giants have compositions spanning the interval $[\text{Fe}/\text{H}]$ from -0.17 to $+0.42$ with a mean value of $+0.15$ and relative elemental abundances $[\text{El}/\text{Fe}]$ representative of the Galactic thin disc. Selection effects may have biased the selection from the *Hipparcos* catalogue against the selection of metal-poor stars. Our reconsideration of the recent extensive survey of FG dwarfs which included metal-poor stars (Bensby et al. 2014) provides a $[\text{Fe}/\text{H}]$ distribution for the Hercules stream which is similar to that from the 58 giants. It appears that the stream is dominated by metal-rich stars from the thin disc. Suggestions in the literature that the stream includes metal-poor stars from the thick disc are discussed.

Key words: stars: abundances — stars: moving groups— Galaxy: kinematics and dynamics—Galaxy: disc

1 INTRODUCTION

The local Milky Way disc is resolvable into two principal large-scale components – the thin and the thick disc – with distinct differences in chemical composition, kinematics and stellar ages. Within the disc there are open clusters comprised of stars of a common age and composition moving together around the centre of the Galaxy. These clusters are not permanent features but disperse due to their internal velocity dispersion and interaction with the gravitational field of the Galaxy: see, for example, Feltzing & Holmberg (2000). Dissolution of clusters feeds the population of field stars within the disc. Other aggregations of stars within the disc have been identified through their common kinematics. Various labels – moving groups, stellar streams and superclusters – have been applied to collections of such kinematically-associated stars. Modern investigations of these entities began with Eggen (1958a, b and c) who supposed that a moving group was a dissolving open cluster (see Eggen 1996 and references therein). Today, proposed origins of stellar streams include not only this early idea of a dissolving cluster but the possibility that some may be remnants of an accreted dwarf satellite galaxy (Navarro, Helmi & Freeman 2004) and that others are collections of field stars with common kinematics arising from dynamical perturbations

within the Galaxy including the effects of the spiral arms (e.g., Quillen & Minchev 2005) and/or the central bar (Fux 2001). For fuller discussion of possible origins of the stellar streams see Antoja et al. (2010) and Sellwood (2014).

A kinematic search for stellar streams and determination of stream members follows Eggen's pioneering ideas and involves quantitative scrutiny of the Galactic motions (U, V, W), where U , V and W are the radial, tangential and vertical components of velocity. In assigning membership of a stream, the three components may be considered directly or in simple combinations. With the publication of the *Hipparcos* catalogue, several authors compiled (U, V, W) components for various stellar samples. In Figure 1, we show the U, V -plane for local K and M giants as presented by Famaey et al. (2005, their Figure 9). Their sample of about 6000 giants, all north of the celestial equator and believed to be single stars, was sorted by a maximum likelihood method into several classes including the three most striking moving groups – Hyades-Pleiades, Sirius and Hercules streams – as well as young giants, high-velocity (thick disc and halo) giants and a group of about 4000 background (mostly thin disc) giants. The fractions of the 6030 stars assigned to the streams are 7.0%, 5.3% and 7.9% for the Hyades-Pleiades, Sirius and Hercules streams, respectively. This paper is devoted to the chemical compositions of those stars assigned to the Hercules stream.

Eggen (1958a and c), based on a set of 700 high-velocity

* E-mail: ramya09@gmail.com

stars identified a number of stars with kinematic motions similar to ζ Herculis, a bright star in the Hercules constellation. Hence, the group is called the Hercules stream. A major characteristic of the Hercules stream in the solar neighbourhood is its negative U velocity, i.e., it is moving outward from the Galactic centre. In a 2008 paper (Famaey et al. 2008) based on a wavelet approach, the Hercules stream – the green elongated structure in Figure 1 – was resolved into two clumps corresponding to U from -65 to -49 km s $^{-1}$ and U from -40 to -30 km s $^{-1}$, both with V from -55 to -47 km s $^{-1}$. In an analysis of Famaey et al.’s sample of giants and of the Geneva-Copenhagen survey of 14,000 dwarfs (Nordström et al. 2004), Zhao, Zhao & Chen (2009) identified 22 moving groups including the Hercules stream. (Throughout this paper unless otherwise stated, velocities U, V, W are heliocentric values.)

Our principal goal is to present abundance analyses of giants from Famaey et al.’s list of very probable members of the Hercules stream. In the following section (Section 2), we discuss the sample and our spectroscopic observations. Section 3 covers the abundance analysis, the elemental abundances, stellar ages and kinematics. Section 4 discusses our abundances in the context of the compositions of the Galactic thin and thick discs as well as previous determinations of the compositions of Hercules stream members, notably that by Bensby et al. (2007, 2014) for dwarf members of the stream. The concluding Section 5 summarizes our principal results concerning the nature of the Hercules stream.

2 SAMPLE AND OBSERVATIONS

Our sample of giants was chosen from Famaey et al. (2005). By applying a maximum-likelihood method to the kinematic data of more than 6000 K and M giants (excluding binaries) they grouped their sample into a number of substructures (Figure 1) and identified 529 stars as belonging to the Hercules stream with 204 given a high probability ($> 70\%$) of membership in the stream. It was this latter subset that forms the basis of our sample. To avoid very cool stars with complex spectra and to restrict the sample to stars with atmospheric parameters similar to the bright K giant star, Arcturus, we chose stars with the colour cut off $V - I < 1.2$. Further, this sample of 140 stars was culled to be accessible from the Harlan J. Smith 2.7 m Telescope at the W.J. McDonald Observatory at the time of our observing runs.

Spectra of 58 giants in the Hercules stream were obtained using the Robert G. Tull coude spectrograph (Tull et al. 1995) at the Harlan J. Smith Telescope. Observed spectra cover the wavelength range: 3800-10000 Å. However, beyond ~ 5800 Å, coverage is incomplete owing to gaps between the recorded portions of the spectral orders which progressively increases towards redder wavelengths. At a resolving power of $\sim 60,000$, the observed spectra have a S/N of 100 or more over much of the spectrum. Spectral images were reduced to one dimensional flux versus wavelength using the software Image Reduction and Analysis Facility (IRAF).¹

¹ IRAF is distributed by the National Optical Astronomy Observatory, which is operated by the Association of Universities for Research in Astronomy (AURA) under cooperative agreement with the National Science Foundation.

The pre-processing tasks such as the bias and flat corrections, wavelength calibration using ThAr lamp spectrum, scattering correction, continuum fitting and Doppler correction were performed on the data.

3 ANALYSIS

In this section, we describe photometric and spectroscopic estimations of atmospheric parameters, the derivation of elemental abundances, ages and kinematical properties of the observed giants from the Hercules stream.

3.1 Stellar Atmospheric Parameters

Atmospheric parameters effective temperature T_{eff} , surface gravity $\log g$, microturbulence ξ_t and metallicity $[M/H]$ were obtained for each star using spectral line analysis combined with stellar models. For deriving atmospheric parameters we used convective stellar model atmosphere with no convective overshoot (Kurucz 1998) and the 2009 version of the LTE line analysis code MOOG (Snedden 1973). Line data were taken from the compilations of Reddy et al. (2003) and Ramírez & Allende Prieto (2011).

An iterative method of spectroscopic estimation of the stellar atmospheric parameters was followed. The first step in this process is to choose an element with numerous lines in the spectra and having a good range in line strengths, lower excitation Potential (LEP) and also having adequate numbers of both neutral and ionized lines. The element Fe satisfying these conditions was chosen and Table 1 gives the list of Fe I lines (LEP in the range of 0-5 eV) and Fe II lines used in the analysis. The effective temperature was set by the requirement that the Fe abundance provided by Fe I lines be independent of their LEPs. This was achieved by forcing the slope of Fe I abundances versus LEPs plot to be zero. ξ_t is derived based on the fact that it affects lines of different strengths differently. The weak lines are unaffected by microturbulence while the strong lines are highly affected. ξ_t is fixed such that Fe I abundances are independent of their line strengths by demanding the slope of the abundances versus $\log(W_\lambda/\lambda)$ plot be zero. As the number of Fe II lines were fewer than for Fe I lines, less weightage was given to them while deriving T_{eff} and ξ_t . Also, while deriving T_{eff} , care was taken to minimize the effect of ξ_t by choosing, initially very weak lines with a sufficient range in LEP. Later, ξ_t was fixed by adding moderately strong Fe I lines. The surface gravity $\log g$ was obtained by requiring that for the given T_{eff} and ξ_t , Fe I and Fe II lines give the same abundance. This mean abundance of Fe is considered to be the metallicity $[M/H]$. Derived parameters based on the spectroscopic analysis are given in Table 2.

The uncertainties of the estimated values of stellar atmospheric parameters are found by checking systematically, how the Fe abundances used for their determination respond to the changes in their values. To find the uncertainty in T_{eff} , the temperature was varied in steps of ± 25 K by keeping all other parameters - $\log g$, ξ_t and $[M/H]$ - constant; for a change of ± 50 K, the slope of the Fe I abundance versus LEP plot changed appreciably. The uncertainty in $\log g$ was estimated by varying the $\log g$ value keeping T_{eff} , ξ_t and

[M/H] constant, until the Fe II abundance differed noticeably from the Fe I abundance value; this led to a measured uncertainty of ± 50 K and ± 0.2 cm s $^{-1}$ in T_{eff} and $\log g$, respectively. A similar analysis by changing the ξ_t , keeping the other parameters constant gave an uncertainty of ± 0.2 km s $^{-1}$ in ξ_t , corresponding to a visually detectable slope to the Fe I abundance versus $\log(W_\lambda/\lambda)$ plot. These individual uncertainties translate to an effective error of ± 0.1 dex in metallicity. It should be noted that the errors in the stellar parameters are not uncorrelated, as the same lines or subsets of the same set of lines are used to derive all of them. This exercise was done for a representative star HIP 8926 and the estimated uncertainties in model parameters are representative of all the stars in our sample.

Derived spectroscopic values of T_{eff} and $\log g$ were checked against those derived using photometry. T_{eff} values were derived using empirical calibrations of optical and infrared photometry. Two colours $J - K$ and $V - K$ and the colour-temperature relations given in Alonso, Arribas & Martínez-Roger (1999) were used. Magnitudes of J and K were taken from 2MASS sky survey (Cutri et al. 2003). The 2MASS magnitudes were converted to the standard TCS system using the calibration given in Ramírez & Meléndez (2005). The V magnitude in $V - K$ was taken from Tycho2 catalogue. Values of V_T magnitudes in the Tycho2 catalogue, were converted to Johnson broad band magnitude V using the relation provided in the Tycho2 catalogue. The K_s magnitudes in 2MASS were converted to K magnitudes of the Johnson system using the relation in Bessell (2005). Magnitudes were corrected for interstellar extinction using the relations given in Ramírez & Meléndez (2005). We assumed $[\text{Fe}/\text{H}] = 0$ for relations that contain the $V - K$ colour. Derived T_{eff} values from $J - K$ and $V - K$ colour are given in Table 2, and are compared in Figure 2. An error of 40 K and 125 K respectively, are associated with the photometric temperatures $(T_{\text{eff}})_{V-K}$ and $(T_{\text{eff}})_{J-K}$ estimated using $V - K$ and $J - K$ colour respectively. Spectroscopic and photometric temperatures agree quite well but problems exist for the coolest stars. For the warmer stars, the photometric temperatures are about 200 K cooler than the spectroscopic values.

The surface gravities ($\log g$) were obtained through web interface (PARAM code²) for the Bayesian estimation of stellar parameters (see da Silva et al. 2006 for details), using the PARSEC isochrones (Bressan et al. 2012). The log-normal initial mass function from Chabrier (2001) and a constant star formation rate were assumed as Bayesian priors. As input parameters, $(T_{\text{eff}})_{\text{spec}}$, $[\text{Fe}/\text{H}]$, parallax (van Leeuwen 2007) and dereddened V magnitude were used. Note that, we derived extinction values $E(B-V)$ using the extinction maps of Schlegel et al. (1998) and the recipes provided in Bonifacio et al. (2000). Derived values are tabulated in Table 2 and are compared in Figure 2. As shown in the Figure, $\log g$ values from photometry are systematically lower by about 0.2 dex compared to values from spectroscopy, which is consistent with the results given in da Silva et al. (2006). Given the uncertainties in the parallaxes, photometry and the spectroscopic determination, the agreement between the two methods is satisfactory. In this

study, we used the atmospheric parameters derived from the spectroscopy.

3.2 The Elemental Abundances

In this section, we present abundances of 15 elements for the 58 giants of the Hercules stream and compare results with those from two independent and smaller surveys of Hercules giants also extracted from the Famaey et al. sample.

The measured lines and adopted atomic data are given in Table 3. Abundances were derived using the Kurucz stellar model atmospheres and the LTE line analysis code *MOOG*. Our reference solar abundances were derived using the solar spectrum taken from Hinkle et al. (2000). The measured equivalent width of each line and the estimated abundances from these lines in Sun are given in Table 3. The standard spectroscopic procedure as outlined in section 3.1 was used to obtain solar atmospheric parameters : $T_{\text{eff}} = 5835$ K, $\log g = 4.55$ cm s $^{-2}$, $\xi_t = 1.25$ km s $^{-1}$ for the metallicity $[\text{M}/\text{H}] = 0$. The derived solar abundances along with the literature values (Asplund et al. 2009) are given in Table 4. Our and the literature results agree within the estimated uncertainties. Derived abundances for the 58 Hercules giants are given in Table 5 and Table 6 in the form $[\text{Fe I}/\text{H}]$, $[\text{Fe II}/\text{H}]$ and then $[\text{El}/\text{Fe}]$ with two entries for $[\text{Ti}/\text{Fe}]$: one for $[\text{Ti I}/\text{Fe}]$ and another for $[\text{Ti II}/\text{Fe}]$. The Ti entries provide a check on the spectroscopic $\log g$ which is based on equality of the Fe abundances from Fe I and Fe II lines. The mean difference $[\text{Ti I}/\text{Fe}] - [\text{Ti II}/\text{Fe}]$ is a satisfactory -0.02 with a hint of more positive values or a larger scatter at the coolest effective temperatures.

Hyperfine corrections were applied for the elements Mn, Co, Sc and V using the wavelengths and relative strengths of hyperfine components taken from the Kurucz database. Ba lines are affected by both hyperfine and isotopic splitting. Ba has seven isotopes ^{130}Ba , ^{132}Ba , ^{134}Ba , ^{135}Ba , ^{136}Ba , ^{137}Ba and ^{138}Ba contributing 0.106 %, 0.101 %, 2.417 %, 6.592 %, 7.854 %, 11.23 % and 71.70 % of the total solar system Ba abundance respectively (Anders & Grevesse 1989). We adopted the wavelength and relative strength of Ba components from McWilliam (1998). The Zn abundance was based initially on the transitions at 4810.54 Å and 6362.35 Å. However, measurement of W_λ of the transition at 4810.54 Å was found to be unreliable for some stars as one wing overlaps with Fe II and/or Cr I lines (Hinkle et al. 2000). Thus, we list Zn abundance only when both the lines were measured.

The error in the mean abundance can be statistically represented as $\bar{\sigma} = \sigma/\sqrt{N}$, where σ represents the standard deviation or the line to line spread in the abundances and N is the number of lines used for the abundance estimation (see Table 5 and 6 for the values). But, the systematic uncertainties associated with the estimated stellar parameters and with the atomic data and measured equivalent width of the spectral lines, get propagated to the estimated abundance value, and exceed the $\bar{\sigma}$ in most of the cases. The resultant uncertainty in the abundances due to any parameter is gauged by measuring the amount by which the mean abundances vary responding to a change in the respective parameter by an amount equal to the uncertainty in the parameter. Following the method, the resultant uncertainties in the abundances, $\sigma(T_{\text{eff}})$, $\sigma(\log g)$, $\sigma(\xi_t)$ and $\sigma([\text{M}/\text{H}])$ due to the uncertainties in the atmospheric parameters - $\Delta(T_{\text{eff}})$

² http://stev.oapd.inaf.it/cgi-bin/param_1.3

± 50 K in temperature, $\Delta(\log g) = \pm 0.20$ cm s⁻² in surface gravity, $\Delta(\xi_t) = \pm 0.20$ km s⁻¹ in microturbulent velocity and $\Delta([M/H]) = \pm 0.10$ dex in metallicity respectively, were estimated. The atomic data we are mainly concerned with are the $\log gf$ values, which are carefully chosen from literature. Moreover, errors in gf -values get cancelled out in the differential abundance analysis with respect to Sun, as the same lines with same atomic data are used for both. The uncertainty in the measured W_λ is estimated using the recipe given in Cayrel (1988) and it turned out to be in the range from 1mÅ to about 2.5mÅ for our data. On average, the uncertainty in the measured W_λ is taken to be $\Delta(W_\lambda) = \pm 2$ mÅ. As there are N lines used for the analysis, the quantity $\bar{\sigma}(W_\lambda) = \sigma(W_\lambda)/\sqrt{N}$ represents the error in abundances due to $\Delta(W_\lambda)$. Although these uncertainties are not uncorrelated, assuming them to be so, they are added in quadrature to get the total systematic error in the abundances.

The above procedure was applied to a typical member (HIP 8926) of our Hercules stream sample and the results are given in Table 7. Assuming that the uncertainties in the parameters are unrelated and independent, the net uncertainty in the abundance ratio was calculated as a quadratic sum which is given in the last column in Table 7 as σ_{model} . Abundance ratios of singly ionised species Ti II, Fe II and Ba II were found to have large uncertainties due to their higher sensitivity to uncertainties in $\log g$ and ξ_t .

Two recent independent studies have analyzed Hercules giants from the Famaey et al. sample using high-resolution spectra of a similar quality to ours, similar analytical techniques but independent selections of lines. These provide an external check on our results. Pakhomov, Antipova & Boyarchuk (2011) obtained spectra of 17 giants of which 11 are in common with our sample. Their selected giants have a greater than 80% probability of belonging to the Hercules stream. Liu et al. (2012) observed 10 giants of which two are in common with us. Pakhomov et al. and Liu et al. have no stars in common.

For the Pakhomov et al. sample, differences in abundance between the two studies ($\Delta[X/H] = \text{current value} - \text{Pakhomov value}$) for common stars are given in Table 8. Agreement is, in general, satisfactory except for one or two of the 11 common stars. For example, for HIP 107502 the abundance values are systematically higher in our study. This is likely due to our higher value of T_{eff} by 290 K and $\log g$ by 1.1 dex compared to Pakhomov et al. (2011). Also, one notices significantly higher values of Mn and Co for most of the stars in our study. It is not clear whether the difference is due to different $\log gf$ -values or to differing treatment of HFS in the two studies. Pakhomov et al. (2011) considered HFS splitting for Co but not for Mn. We include HFS for both these elements. Additionally, there is incomplete overlap in the lines of Mn I and Co I chosen for the two abundance analyses. There are large differences for Ba II. A major contributor here is that the $\log gf$ -values adopted by Pakhomov et al. are 0.2 dex larger than our values for the two lines we use to obtain the Ba abundance. Pakhomov et al.'s sample have a probability of greater than 80% of belonging to the Hercules stream; recall that our sample was chosen to have a probability of 70% or greater.

For the two stars in common with Liu et al., the mean difference for $[X/Fe]$ from 11 common elements is 0.03 for

one (HIP 51047) and 0.02 for the other star (HIP 37441) with 10 of 11 or 9 of the 11 $[El/Fe]$ falling within ± 0.10 dex. The $[Fe/H]$ values differ by 0.11 dex for HIP 51047 and 0.09 dex for HIP 37441 in the sense that our values are larger. In part the $[Fe/H]$ differences are likely attributable to our hotter T_{eff} and stronger surface gravity. Liu et al. adopted a looser criterion for membership than either ourselves or Pakhomov et al.; the probabilities for membership are as low as 45% and 46% for two stars and only four of their ten stars meet our criterion of a probability of 70% or greater.

The histogram for $[Fe/H]$ for our 58 giants is shown in Figure 3. The sample spans the $[Fe/H]$ range from -0.17 to $+0.43$ with a peak at $[Fe/H] = +0.15$. A characteristic of the stream is its spread in U (Figure 1) but the composition of the stream's giants does not appear to depend on U ; stars with $U < -50$ km s⁻¹ and those with $U > 50$ km s⁻¹ share the same $[Fe/H]$ as the total sample and the two samples are not distinguishable by their $[El/Fe]$. The $[Fe/H]$ distribution is quite similar to that from Pakhomov et al.'s sample: their mean $[Fe/H]$ from 17 stars is $+0.11$. Liu et al.'s quartet of stars with a 70% or greater probability of stream membership have $[Fe/H]$ of -0.36 , -0.26 , -0.25 and 0.0 for a mean of -0.22 which, if we adjust by the 0.1 difference between their and our results from two common stars (see above), gives a mean of -0.12 a value not too severely different from our mean value. In summary, these two independent analyses of Hercules giants provide compositions generally similar to results from our larger sample.

Two characteristics of Figure 3 surely deserve comment. First, metal-poor stars, say $[Fe/H] \leq -0.5$ are absent. Second, observed stars span a $[Fe/H]$ range much greater than the measurement uncertainty and, therefore, indicate that the Hercules stream is not a dissolving open cluster. A contributing factor to the absence of metal-poor stars may be a selection effect embedded in the Famaey et al. sample (2005). Their principal selection criteria were that a star must have a spectral type of K or M in the *Hipparcos* input catalogue and then an absolute magnitude limit was imposed to separate the K (and M) giants from dwarfs. Given that evolutionary tracks for giants move to the blue and earlier spectral types with decreasing metallicity, metal-poor giants will not have been selected by Famaey et al. The cut-off as the spectral type moves to G-type for giants probably occurs at slightly less than $[Fe/H]$ of -0.5 ; Arcturus with $[Fe/H] \simeq -0.5$ has a spectral type of K2IIIp in the *Hipparcos* catalogue. Secondly, the local density of metal-poor field stars is low and, if a stream's population even approximately mirrors that of the field, very large or targeted samples are surely required in order to locate metal-poor stars in the Hercules stream. The density of metal-poor giants in a distance-limited sample such as the *Hipparcos* catalogue is likely lower than for metal-poor dwarfs because of the shorter lifetime of a giant. In short, absence of metal-poor giants in the Hercules stream as selected by Famaey et al. (2005) likely arises from selection effects and may not be an intrinsic property of the stream. Such selection effects may be mitigated and even eliminated by surveys selected by U, V, W velocities.

Confirmation of a metallicity distribution centred at about the solar metallicity is provided by two analyses which draw a large fraction of their stellar sample from the Geneva-Copenhagen survey of FGK dwarf stars (Nordström et al.

2004; Holmberg, Nordström & Andersen et al. 2007). Antoja et al. (2008) identify a sample of Hercules stream members among the more 10000 FGK dwarfs with (U, V) values very similar to those isolated by Famaey et al. (2005). With Strömgren metallicities from the Geneva-Copenhagen catalogue, Antoja et al. (their Table 4 and Figure 15) give the mean $[\text{Fe}/\text{H}]$ as -0.15 ± 0.27 . Bobylev, Bajkova & Mylläri (2010) with a sample of more than 15000 stars identify almost 200 stars with the Hercules stream distributed among two clumps coincident with Famaey et al.’s identification of the stream in Figure 1. Mean metallicities, again from Strömgren metallicities, are $[\text{Fe}/\text{H}] = -0.09 \pm 0.17$ for the clump at $(U, V) = (-33, -51)$ and -0.16 ± 0.27 for the clump at $(U, V) = (-77, -49)$ and these values not surprisingly are consistent with those from Antoja et al. Even these two samples provide too few members of the Hercules stream to contain metal-poor stars.

3.3 Ages

Ages of individual stars were estimated using the PARAM code and PARSEC isochrones (Bressan et al. 2012) with Bayesian priors for the Initial mass function (the lognormal function from Chabrier 2001) and the Star Formation Rate (constant). Essential background to the PARAM code is provided by da Silva et al. (2006) who remark that derived quantities such as the mean stellar age and its standard error are derived from a probability distribution function for the logarithm of the age. Spectroscopic effective temperature and $[\text{Fe}/\text{H}]$ were used as input along with van Leeuwen’s revised *Hipparcos* parallax and the reddening corrected V magnitude. Ages and error estimates are given in Table 2. A histogram of stellar ages is shown in Figure 4. Except for two outliers (HIP 7710 at 6.1 ± 2.8 Gyr and HIP 48417 at 7.1 ± 2.6 Gyr), the ages are less than 4 Gyr with a peak around 1.5 Gyr. The width of the histogram exceeds typical errors and, thus, confirms that the stream is not a dissolved open cluster. These ages are typical of local thin disc stars (Bensby et al. 2005, 2014; Reddy et al. 2003) and not of the local thick disc for which far greater ages have been derived, as, for example, the 10.7 Gyr by Reddy et al. and 9.7 Gyr by Bensby et al.

Age estimates for common stars were compared with Pakhomov et al. (2011) who estimated ages from isochrones (Girardi et al. 2000) and a star’s location in the $\log L/L_\odot$ versus T_{eff} plane. Agreement with our estimates is very good except for two stars: HIP 107502 where our age is much shorter and HIP 108012 where our age is much longer than estimates given by Pakhomov et al. For the former case, a possible explanation is that our effective temperature is nearly 300 K warmer which reduces the age and also brings the abundances into agreement.

Ages have also been estimated for FG dwarfs identified with the Hercules stream. With age estimates for stars in the Geneva-Copenhagen survey derived from Strömgren photometry and a Bayesian estimation technique, Antoja et al. (2008) found an age distribution peaking at 2.2 Gyr with a full-width and half power of about 1.2 Gyr with a low density tail extending to at least 8 Gyr (see their Figure 17). This age profile is similar to that illustrated in Figure 4. Adopting age estimates from Holmberg et al. (2007), Bobylev et al. (2010) quote ages of around 5 Gyr with an uncertainty

of about 3 Gyr for both cores of the Hercules stream. These estimates appear incompatible with those from Antoja et al. and our values as summarized in Figure 4.

3.4 Kinematics and Stream Membership

In light of van Leeuwen’s (2007) revisions to the *Hipparcos* astrometry, we decided to recalculate the motions (U, V, W) of our giants. Radial velocities were estimated from our spectra by cross-correlation with a template spectrum. The typical error in radial velocity is $\pm 1 \text{ km s}^{-1}$. The measured radial velocities in this study agree well with those given by Famaey et al. (2005); the mean difference (ours - them) is $+0.47 \pm 1.25 \text{ km s}^{-1}$. Space velocities (U, V, W) were derived using the recipe given in Johnson & Soderblom (1987) combined with new radial velocities and the updated *Hipparcos* astrometry. The mean differences between the values derived in this study and those given Famaey et al. (2005) are small: -1 ± 8 , 0.3 ± 7 and $0.2 \pm 3 \text{ km s}^{-1}$, respectively for U , V and W . These small differences have no more than a minor effect on the selection of Hercules stream members from Famaey et al.’s catalogue.

Crucial to the identification of members of the Hercules stream is the procedure for isolating stream members from other stars in the (U, V) plane and/or other diagrams involving the (U, V, W) velocities or quantities derived from these velocity components. Our sample of giants drawn from Famaey et al. (2005) adopts their probability estimates for stream membership based on the mean stream velocities of $(U, V, W) = (-42, -52, -8)$ and their $(\sigma_U, \sigma_V, \sigma_W)$ - see their Table 2 for a full specification of the parameter set including the fraction of their total sample assigned to the Hercules stream and to the other components (see above): $7.9 \pm 0.9 \%$ of the 6030 stars are assigned to the Hercules stream. Our selection criterion was that stars must have a 70% or greater probability of belonging to the Hercules stream, as estimated by Famaey et al. (2005). It is assumed that Famaey et al.’s (2008) subsequent resolution of the U distribution of the Hercules stream into two clumps (U from -49 to -65 km s^{-1} and -30 to -40 km s^{-1} with V from -47 to -55 km s^{-1}) does not greatly affect the probability of stream membership. Probability calculations performed by Famaey et al. (2005, 2008) are similar but not exactly equivalent to the calculations for Galactic entities described by Bensby et al. (2003), Reddy et al. (2006) and Bensby et al. (2014) based on Gaussian distribution functions for the different entities. Use of Reddy et al.’s (2006) recipe with Famaey et al.’s (2005) parameters for their six populations overestimates the probability that a star belongs to the Hercules stream but by only a few per cent.

4 THE HERCULES STREAM AND THE GALACTIC DISC

In essentially all respects, the composition of the Hercules giants is identical to that of thin disc giants in the solar neighborhood. Luck & Heiter’s (2007) abundance analyses of a large sample of local GK giants is our reference sample. The vast majority of their giants belong to the thin Galactic disc; discussion of possible differences between thin and

thick disc stars is given below. In terms of the $[\text{Fe}/\text{H}]$ distribution, Luck & Heiter's sample has a mean value $[\text{Fe}/\text{H}] = 0.0$ and a sharp cutoff at $[\text{Fe}/\text{H}] \simeq +0.3$ and a low $[\text{Fe}/\text{H}]$ tail extending to -0.6 . Our sample of giants has a higher mean $[\text{Fe}/\text{H}]$ ($= +0.15$) and a higher fraction of high $[\text{Fe}/\text{H}]$ stars than this local field sample and, as noted above, a distinct paucity of metal-poor stars which likely results in part from the selection effects inherent in the Famaey et al. (2005) sample. (A sample of local FGK dwarfs analyzed by Luck & Heiter (2006) has a more pronounced high $[\text{Fe}/\text{H}]$ tail and closely resembles our histogram for $[\text{Fe}/\text{H}] \geq 0.0$.) With the possible exception of our higher fraction of 'very' metal-rich stars, the $[\text{Fe}/\text{H}]$ distribution for Hercules giants resembles that of local giants. An excess of high metallicity stars among the Hercules stream may imply origins in the inner Galaxy where metallicities are higher at about the gradient of 0.1 dex kpc^{-1} according to measured abundance gradients. As noted above, metal-poor giants are probably underrepresented in these histograms.

The concordance between $[\text{Fe}/\text{H}]$ distributions for Hercules and local field giants extends to element ratios $[\text{El}/\text{Fe}]$. In Table 9, we give $[\text{El}/\text{Fe}]$ for the three $[\text{Fe}/\text{H}]$ intervals: $[\text{Fe}/\text{H}] = -0.2$ to 0.0 , 0.0 to $+0.2$ and $+0.2$ to $+0.4$ for our sample of Hercules giants and Luck & Heiter's (2007) field giants. Inspection of Table 9 shows a close correspondence between $[\text{El}/\text{Fe}]$ values in the two samples across the full $[\text{Fe}/\text{H}]$ interval. This is further illustrated in Figures 5 and 6. Figure 5 shows $[\text{Na}/\text{Fe}]$ versus $[\text{Fe}/\text{H}]$ for the Hercules giants, Luck & Heiter's (2007) giants and FG dwarfs from Bensby et al. (2014). Figure 6 shows $[\text{Mg}/\text{Fe}]$, $[\text{Si}/\text{Fe}]$ and $[\text{Ni}/\text{Fe}]$ versus $[\text{Fe}/\text{H}]$ for our sample of Hercules giants and local giants from Luck & Heiter (2007). Slight differences in $[\text{El}/\text{Fe}]$ may arise from differences in analytical techniques but the impression is that the $[\text{El}/\text{Fe}]$ values for the Hercules stream are the same as those for local field giants which represent the Galactic thin disc.

Several discussions of the Hercules stream have suggested that the stream has a component from the Galactic thick disc. Differences in composition between thin and thick discs are most obvious at low $[\text{Fe}/\text{H}]$, say $[\text{Fe}/\text{H}] \leq -0.3$, where, in particular, the abundances of α -elements Mg, Si, Ca and Ti are enhanced in the thick relative to the thin disc with $[\alpha/\text{Fe}] \simeq +0.3$. Differences between thin and thick discs decrease as $[\text{Fe}/\text{H}] = 0$ is approached. The local thick disc is represented by stars with $[\text{Fe}/\text{H}]$ as low as -1.2 and extends up to 0.0 (Bensby et al. 2007) and possibly to $+0.2$ (Bensby et al. 2014). The interval $[\text{Fe}/\text{H}] \simeq 0.0$ is populated also by a class of stars dubbed high- α metal-rich (HAMR) stars introduced by Adibekyan et al. (2011) who proposed that HAMR stars formed a separate population in the local disc. Bensby et al. (2014), on the other hand, suggest HAMR stars are simply the metal-rich extension of the thick disc. For our present purpose, the relation between the HAMR stars and the metal-rich thick disc is academic. What is key is that there are differences between the composition of thin and of thick/HAMR stars at the same $[\text{Fe}/\text{H}]$ but such differences diminish as $[\text{Fe}/\text{H}] = 0$ is approached from low $[\text{Fe}/\text{H}]$. This merger is shown in Figure 7 for $[\text{Ti}/\text{Fe}]$ where results for our Hercules giants are shown with results for 'certain' thin and thick disc dwarfs from Bensby et al. (2014). For $[\text{Fe}/\text{H}] \leq 0.0$, a thick (HAMR) – thin disc separation is present and the Hercules giants favour the thin

disc. Note that high $[\text{Ti}/\text{Fe}]$ and low $[\text{Ti}/\text{Fe}]$ loci are not populated purely by kinematically-selected thin and thick disc stars, respectively; this mixing suggests either the labels 'thin' and 'thick' are misapplied in some cases and/or the indices $[\text{Ti}/\text{Fe}]$ and $[\alpha/\text{Fe}]$ are not a guaranteed identifier of a population. Bensby et al.'s Figure 23 which shows $[\text{Ti}/\text{Fe}]$ versus $[\text{Fe}/\text{H}]$ with stars differentiated by their high or low $[\text{Ti}/\text{Fe}]$ value for each $[\text{Fe}/\text{H}]$ value shows the HAMR stars with $[\text{Ti}/\text{Fe}]$ excesses of about 0.15 , 0.05 and 0.0 dex at $[\text{Fe}/\text{H}]$ of -0.2 , 0.0 and $+0.2$ dex, respectively, over thin disc stars with $[\text{Ti}/\text{Fe}]$ of close to 0.0 . By a very large majority, the Hercules giants in Figure 7 fall with the thin disc and not the HAMR stars. A cautionary note: the HAMR-thin disc abundances from Bensby et al. and Adibekyan et al. are derived from standard analyses of warm dwarfs but our results are for giants of cooler temperatures and, hence, systematic differences in $[\text{El}/\text{Fe}]$ might intrude into Figure 7. Luck & Heiter's (2006, 2007) standard analyses of such dwarfs and giants show that differences are small and, in addition, standard analyses of dwarfs by Luck & Heiter and by Bensby et al. are in fine agreement (Reddy, Giridhar & Lambert 2015 – their Table 16). Across the $[\text{Fe}/\text{H}]$ interval covered by the Hercules stream giants, their compositions indicate that they closely resemble thin disc stars rather than the thick disc/HAMR stars.

The presence of thick disc stars, especially metal-poor examples, within the Hercules stream was advocated by Bensby et al.'s (2007) who concluded that the Hercules stream was not 'a unique Galactic stellar population but rather is a mixture of thin and thick disc stars' and this claim was reinforced by Bensby et al. (2014) who tightened their 2007 criteria for stream membership: the 2014 criteria for stream membership were that the kinematic probabilities of membership in the thin disc (D), thick disc (TD) and the Hercules stream (Her) should satisfy the constraints $Her/D > 2$ and $Her/TD > 2$ but in the 2007 paper the criteria were that these two ratios should be greater than one. However, the tougher criteria for membership did not materially alter the range in composition of the stars identified with the Hercules stream. The 2014 sample of some 30 members range in $[\text{Fe}/\text{H}]$ from -0.9 to $+0.3$ with almost all of the stars having $[\text{Fe}/\text{H}] \leq -0.2$ and the α -element enhancement ($[\alpha/\text{Fe}] \geq +0.1$) characteristic of the thick disc. One might suggest that the Bensby et al. (2014) sample of the Hercules stream arises *in toto* from the thick disc!

This sample's composition contrasts sharply with ours: we have no stars more metal-poor than $[\text{Fe}/\text{H}] \simeq -0.2$ and their relative abundances $[\text{El}/\text{Fe}]$ are typical of the thin disc. The contrast is not traceable to the fact that one analysis refers to dwarfs and the other to giants. Rather, it arises from different (U, V, W) definitions for the Hercules stream. Bensby et al. (2007, 2014) centre the stream at $(U, V) = (-51, -62)$ which is about 10 km s^{-1} more negative in U and V than the Famaey et al. (2005 – see the green swath

in Figure 1) values and the consensus of pre- and post-2005 determinations.³

Given that the stream is stretched out in U but rather tightly confined in V , a crucial quantity in selection of members is the choice of V . A consequence of Bensby et al.'s choice for the (U, V) centroid is that their proposed stream members populate the (U, V) plane about 10 km s^{-1} in V below the green swath identified with the Hercules stream in Figure 1. Thus, Bensby et al. place the stream deeper among the thick disc stars than Famaey et al.'s choice of (U, V) and this, we suspected, explains the large contribution from the thick disc to the Bensby et al. selection of stream members.

To test our suspicion, we interrogated Bensby et al.'s (2014) list of 714 stars using Famaey et al.'s parameters for their six contributors to the local stellar population (see above) and identified 28 stars having a probability of greater than 80% of belonging to the stream. This sample has a narrower $[\text{Fe}/\text{H}]$ range than that selected by Bensby et al. – see Figure 3 where we find our selection from Bensby et al.'s 714 stars has a $[\text{Fe}/\text{H}]$ distribution fairly similar to ours for the Hercules giants. In addition, the relative abundances $[\text{El}/\text{Fe}]$ for the revised sample of Hercules dwarfs are similar to those for our Hercules giants. Notably, the $[\text{Ti}/\text{Fe}]$ for the members from Bensby et al. are overwhelmingly the low values typical of the thin disc. Just three stars have the higher $[\text{Ti}/\text{Fe}]$ with also higher $[\text{Mg}/\text{Fe}]$, $[\text{Si}/\text{Fe}]$ and $[\text{Ca}/\text{Fe}]$ seen among thick and HAMR stars. Each of the three is somewhat Fe-poor ($[\text{Fe}/\text{H}]$ from -0.18 to -0.35). Three thick disc stars out of a sample of 28 is not unexpected given that the selection criterion was a probability of stream membership of 80% or greater. (As noted above, our calculation of probabilities appears to overestimate slightly the probability of stream membership with respect to the probabilities given by Famaey et al. (2005) from their maximum likelihood method.) The age distribution of the 25 low $[\text{Ti}/\text{Fe}]$ stars is consistent with a thin disc origin: 20 stars with reliable ages (see Bensby et al. 2014 who adopt the criterion that the upper and lower estimates of a star's age should not exceed 4 Gyr) provide a mean age of 5.1 Gyr with a distribution from 1.4 Gyr to 10.4 Gyr. Thus, Bensby et al.'s (2014) large sample of FG dwarfs covering a range of metallicities and ages when sifted with appropriate (U, V) confirms that the Hercules stream is predominantly a feature of the thin disc with a majority of members having a near-solar metallicity.

Prior to Bensby et al.'s search for members of the Hercules stream, Soubiran & Girard (2005) assembled data for more than 700 dwarfs and subgiants. By a technique involving Gaussian distribution functions (Bensby et al. 2003, 2014; Reddy et al. 2003) Soubiran & Girard computed a star's probability of belonging to the thin disc, the thick disc and the Hercules stream. Such probabilities rely on the characterization of the Gaussian distribution functions and the relative strength of the three populations. Soubiran & Girard's choice of the Gaussian distribution for the Hercules

stream was taken from Famaey et al. (2005) and for the thin and thick disc from Soubiran et al. (2003). Nearly 600 stars were assigned such probabilities. Just five stars ranging in $[\text{Fe}/\text{H}]$ from -0.90 to $+0.06$ had a probability of greater than 80% of belonging to the Hercules stream and three of the five have α -enhancements typical of the thick disc. If we apply our criterion of a probability of membership of 70% or greater for the Hercules stream, the mean $[\text{Fe}/\text{H}]$ from 21 stars is -0.26 and the distribution is weighted to metal-poor stars more severely than shown by our giants and also by the revised selection from Bensby et al. Of the 21 stars, the great majority belong to the thin disc according to their $[\alpha/\text{Fe}]$ values. Mishenina et al. (2013) who discuss a survey of 276 FGK dwarfs of which slightly more than half were included in Soubiran & Girard's sample reach similar conclusions about the Hercules stream and its mix of thin and thick disc stars.

5 CONCLUDING REMARKS

Our abundance analysis of 58 of the giants assigned to the Hercules stream by Famaey et al. (2005) shows general agreement with Pakhomov et al.'s (2011) independent analysis of 17 of Famaey et al.'s giants. In terms of chemical compositions, the principal results are that (i) the $[\text{Fe}/\text{H}]$ of the 58 giants are spread across the interval -0.15 to $+0.45$ with a mean of $+0.15$ and (ii) the relative abundances $[\text{El}/\text{Fe}]$ for elements such as the α -elements which among the $[\text{Fe}/\text{H}] < 0$ stars are a discriminant between thin and thick disc stars, the results suggest the Hercules stream is composed primarily of thin disc stars. The ages of the Hercules giants average about 1.4 Gyr with a real star-to-star spread. These ages are typical of local thin disc stars (Bensby et al. 2005, 2014; Reddy et al. 2003) and not of the local thick disc for which far greater ages have been derived, as, for example, the 10.7 Gyr by Reddy et al. and 9.7 Gyr by Bensby et al. Not unexpectedly, the spreads in compositions and in ages among stream members exclude the possibility of identifying the stream as a dissolved open cluster.

What was unexpected was the disagreement between our results and published claims that the metallicities of Hercules stream members extended down to $[\text{Fe}/\text{H}] \sim -1$ and contained representatives of both the thin and thick discs. In the case of the most extensive available survey of the compositions of F and G disc dwarfs (Bensby et al. 2014), we argue above that their results for $[\text{Fe}/\text{H}]$ and $[\text{El}/\text{Fe}]$ are quite consistent with ours when the Hercules stream members are selected from among the dwarfs using the same (actually, very similar) criteria as those used by Famaey et al. (2005); Bensby et al.'s (2007, 2014) selection of Hercules stream members were based on inappropriate choices for the stream's central (U, V) velocities. Soubiran & Girard (2005) and Mishenina et al. (2013) also assembled samples of F and G dwarfs and searched their samples for members of the Hercules stream. Their conclusions about the composition of stream members are not as consistent with ours as the adjusted sample from Bensby et al. (2014). In particular, they both conclude that the stream is composed of stars with a much larger $[\text{Fe}/\text{H}]$ spread than we find; there is little to no overlap between the histogram provided by the Hercules giants and that from the high proba-

³ Bensby et al. (2014) give velocities relative to the local standard of rest (LSR). Using their adopted values of Sun's velocity components relative to the LSR, we straightforwardly obtain the heliocentric velocities for their adopted centres of the Hercules stream and velocities for individual stars.

bility dwarf/subgiant members isolated by Soubiran & Girard (2005). There is apparent agreement from composition (i.e., $[\alpha/\text{Fe}]$) and age on the point that the various samples are dominated by thin rather than thick disc stars.

Differences in the $[\text{Fe}/\text{H}]$ spread remain unresolved quantitatively; it is not obviously attributable to the choice of kinematical parameters.⁴ Factors contributing to differences between our sample of the stream and those offered by Soubiran & Girard and Mishenina et al. may be the small number of high probability members from the latter two surveys and the biases in our sample against the inclusion of metal-poor stars. The fact that our sample of stream giants and Bensby et al.'s sample of stream dwarfs drawn from a selection of stars across a wide range in $[\text{Fe}/\text{H}]$ are similar might suggest that the bias inherent in the Famaey et al. (2005) sample is small. Perhaps most curious of all is the observation that the collection of stream members extracted from Bensby et al.'s (2014) large survey of FG stars is so different in terms of their $[\text{Fe}/\text{H}]$ range from that provided by Soubiran & Girard's (2005) almost equally large survey of FG stars and with a quite similar distribution of stars by $[\text{Fe}/\text{H}]$. Such a contrast can not be attributed to systematic differences between abundance analyses nor to the technique from separating stream members from thin and thick disc stars.

Together the compositions, the ages and the kinematics support the picture of the Hercules stream as a flow of stars driven outwards from the inner Galaxy by gravitational perturbations arising from the rotating central bar (see, for example, Fux 2001). The outward flow is not uniform – the U velocities span about 100 km s^{-1} – and unlikely to be steady over long periods because the gravitational perturbations from the Galactic bar and spiral arms are time dependent. (Note that a U velocity of 50 km s^{-1} maintained for 1 Gyr covers a distance of 51 kpc.) Given that our $[\text{El}/\text{Fe}]$ follow closely the thin disc pattern, we suppose that the Hercules stream is a thin and not a thick disc phenomenon, a conclusion confirmed by the estimates of stellar ages. Abundance analyses from the *APOGEE* project show that the inner Galaxy along the Galactic plane is dominated by a thin disc-like (i.e., low $[\alpha/\text{Fe}]$) population with the mean $[\text{Fe}/\text{H}]$ increasing toward the Galactic centre (Hayden et al. 2015). Away from the Galactic plane ($1 < |z| < 2 \text{ kpc}$), a thick disc-like (i.e., high $[\alpha/\text{Fe}]$) population dominates the inner Galaxy with little representation from the thin disc. Paucity of thick disc representatives in the Hercules stream would suggest inefficient mixing in height about the Galactic plane. In contrast to the Hercules stream as a thin disc phenomenon, the two thick disc streams – Arcturus and AF06 – analysed by Ramya et al. (2012) have compositions representative of the thick disc without thin disc contamination. Observational insights into the character of the Hercules stream and novel challenges to a fuller theoretical understanding will come as the Hercules stream is mapped more extensively in distance and azimuth as large surveys are completed, e.g. Antoja et al. (2014) discuss the Hercules stream as seen by

⁴ An idea that an explanation might be found in the fact that the surveys sample different areas of the sky was short-lived. Famaey et al.'s (2005) sample is drawn from stars in the *Hipparcos* catalogue north of the celestial equator. Soubiran & Girard's and Mishenina et al.'s samples, which do not support our abundance results, are heavily weighted to the northern celestial hemisphere while Bensby et al.'s (2014) large sample, which supports our results, is greatly concentrated on the southern celestial hemisphere.

the RAVE survey, and much may be expected from scrutiny of *GAIA* results.

Further insights into the formation and evolution of moving groups and streams may be expected from detailed studies of additional streams in and beyond the solar neighbourhood. Zhao et al. (2009) identified 22 moving groups in the solar neighbourhood. Of this total, few have been subjected to comprehensive abundance analysis. Pursuit of additional moving groups near and far is to be encouraged for as Sellwood (2014) remarks ‘It is likely that the different streams have different origins and a combination of these [theoretical] ideas would be needed to explain all the features.’

6 ACKNOWLEDGMENTS

We are most grateful to the referee for a thorough and constructive report on our initial submission. DLL thanks the Robert A. Welch Foundation of Houston, Texas for support through grant F-634. We thank Alain Jorissen for a helpful exchange of emails concerning Famaey et al.’s selection of Hercules giants and Tamara Mishenina for a clarification about the results from the survey reported by Mishenina et al. (2013).

REFERENCES

- Adibekyan V. Z., Santos N. C., Sousa S. G., Israelian G., 2011, *A&A*, 535, L11
- Alonso A., Arribas S., Martínez-Roger C., 1999, *A&AS*, 140, 261
- Anders E., Grevesse N., 1989. *Geochim. et Cosmochim. Acta*, 53, 197
- Antoja T., Figueras, F., Fernández, D., Torra, J., 2008, *A&A*, 490, 135
- Antoja T., Figueras F., Torra J., Valenzuela O., Pichardo B., 2010, *Lecture Notes and Essays in Astrophysics*, 4, 13
- Antoja, T., Helmi, A., Dehnen, W. et al., 2014, *A&A*, 563, A60
- Asplund M., Grevesse N., Sauval A. J., Scott P., 2009, *ARA&A*, 47, 481
- Bensby T., Feltzing S., Lundström I., 2003, *A&A*, 410, 527
- Bensby T., Feltzing S., Lundström I., Ilyin I., 2005, *A&A*, 433, 185
- Bensby T., Oey M. S., Feltzing S., Gustafsson B., 2007, *ApJ*, 655, L89
- Bensby T., Feltzing S., Oey M. S., 2014, *A&A*, 562, A71
- Bessell M. S., 2005, *ARA&A*, 43, 293
- Bobylev, V.V., Bajkova, A.T., Mylläri, A.A., 2010, *Astr. Letters*, 36, 27
- Bonifacio P., Monai S., Beers T. C., 2000, *AJ*, 120, 2065
- Bressan A., Marigo P., Girardi L., Salasnich B., Dal Cero C., Rubele S. & Nanni A., 2012, *MNRAS*, 427, 127
- Cayrel R., 1988, in Cayrel de Strobel G., Spite M., eds, *The Impact of Very High S/N Spectroscopy on Stellar Physics*. Kluwer Dordrecht, p.345
- Chabrier G., 2001, *ApJ*, 554, 1274
- Cutri R. M., Skrutskie M. F., van Dyk S., Beichman C. A., Carpenter J. M., 2003, *2MASS All Sky Catalog of point sources*.
- da Silva L., Girardi L., Pasquini L., Setiawan J., von der Lüh O., de Medeiros J. R., Hatzes A., Döllinger M. P., Weiss A., 2006, *A&A*, 458, 609
- Eggen O. J., 1958a, *Observatory*, 78, 21
- Eggen O. J., 1958b, *MNRAS*, 118, 65
- Eggen O. J., 1958c, *MNRAS*, 118, 154
- Eggen O. J., 1996, *AJ*, 112, 1595
- Famaey B., Jorissen A., Luri X., Mayor M., Udry S., Dejonghe H., Turon C., 2005, *A&A*, 430, 165
- Famaey B., Siebert A., Jorissen A., 2008, *A&A*, 483, 453
- Feltzing S., Holmberg J., 2000, *A&A*, 357, 153
- Fux R., 2001, *A&A*, 373, 511
- Girardi L., Bressan A., Bertelli G., & Chiosi C., 2000, *A&AS*, 141, 371
- Hayden M. R., Bovy J., Holtzman J. A. et al. 2015, *ApJ*, 808, 132
- Hinkle K., Wallace L., Valenti J., & Harmer D. (ed.) 2000, *Visible and Near Infrared Atlas of the Arcturus Spectrum 3727–9300 Å* (San Francisco, CA:ASP)
- Holmberg J., Nordström, B., Andersen, J. 2007, *A&A*, 475, 519
- Johnson D. R. H., Soderblom D. R., 1987, *AJ*, 93, 864
- Kurucz R.L., 1998, <http://kurucz.harvard.edu/> (online data)
- Liu F., Chen Y. Q., Zhao G., Han I., Lee B. C., Kim K. M., Zhao Z. S., 2012, *MNRAS*, 422, 2969
- Luck R. E., Heiter U., 2006, *AJ*, 131, 3069
- Luck R. E., Heiter U., 2007, *AJ*, 133, 2464
- McWilliam, A., 1998, *AJ*, 115, 1640
- Mishenina T. V., Pignatari, M., Korotin, S. A., et al., 2013, *A&A*, 552, A128
- Navarro J. F., Helmi A., Freeman K. C., 2004, *ApJ*, 601, L43
- Nordström B., Mayor M., Andersen J., Holmberg J., Pont F., Jørgensen B. R., Olsen E. H., Udry S., Mowlavi N., 2004, *A&A*, 418, 989
- Pakhomov Y. V., Antipova L. I., Boyarchuk A. A., 2011, *Astr. Repts.*, 55, 256
- Quillen A. C., Minchev I., 2005, *AJ*, 130, 576
- Ramírez I., Allende Prieto C., 2011, *ApJ*, 743, 135
- Ramírez I., Meléndez J., 2005, *ApJ*, 626, 446
- Ramya P., Reddy B. E., Lambert D. L., 2012, *MNRAS*, 425, 3188
- Reddy, A.B.S., Giridhar, S., Lambert, D.L. 2015, *MNRAS*, 450, 430
- Reddy B. E., Lambert D. L., Allende Prieto C., 2006, *MNRAS*, 367, 1329
- Reddy B. E., Tomkin J., Lambert D. L., Allende Prieto C., 2003, *MNRAS*, 340, 304
- Schlegel D. J., Finkbeiner D. P., Davis M., 1998, *ApJ*, 500, 525
- Sellwood J. A., 2014, *Rev. Mod. Phys.*, 86, 1
- Snedden C., 1973, PhD Thesis, University of Texas, Austin
- Soubiran C., Bienaymé O., Siebert A., 2003, *A&A*, 398, 141
- Soubiran C., Girard P., 2005, *A&A*, 438, 139
- Tull R. G., MacQueen P. J., Sneden C., Lambert D. L., 1995, *PASP*, 107, 251
- van Leeuwen F., 2007, *A&A*, 474, 653
- Zhao J., Zhao G., Chen Y., 2009, *ApJ*, 692, L113

Table 1: Adopted Iron line data

Wavelength Å	LEP eV	$\log gf$	$W_{\lambda_{\odot}}$ mÅ	$\log \varepsilon_{\odot}$ dex
Fe I				
5295.31	4.420	-1.590	29.1	7.53
5358.12	3.300	-3.162	9.5	7.43
5379.57	3.690	-1.510	60.5	7.39
5386.33	4.150	-1.670	32.1	7.43
5441.34	4.310	-1.630	30.3	7.49
5638.26	4.220	-0.770	75.8	7.41
5661.35	4.280	-1.756	21.7	7.38
5679.02	4.652	-0.750	58.2	7.45
5705.46	4.301	-1.355	37.7	7.36
5731.76	4.260	-1.200	56.5	7.52
5778.45	2.588	-3.440	22.2	7.45
5793.91	4.220	-1.619	33.2	7.45
5849.69	3.695	-2.930	6.6	7.38
5855.08	4.608	-1.478	20.9	7.38
5856.10	4.294	-1.558	32.5	7.44
5858.79	4.220	-2.180	12.5	7.44
5859.60	4.550	-0.608	69.3	7.41
5905.67	4.650	-0.690	56.8	7.36
5927.79	4.650	-0.990	41.5	7.38
5929.68	4.550	-1.310	39.5	7.57
6003.01	3.880	-1.060	81.7	7.48
6027.05	4.076	-1.090	63.2	7.35
6056.00	4.730	-0.400	70.6	7.37
6079.01	4.650	-1.020	44.9	7.47
6093.64	4.607	-1.300	30.2	7.42
6096.66	3.984	-1.810	36.9	7.48
6151.62	2.176	-3.282	48.7	7.42
6159.38	4.610	-1.830	12.6	7.45
6165.36	4.143	-1.460	43.9	7.42
6187.99	3.940	-1.620	46.1	7.43
6240.65	2.223	-3.287	47.8	7.45
6270.23	2.858	-2.540	51.6	7.40
6271.28	3.330	-2.703	23.8	7.45
6436.41	4.186	-2.360	10.0	7.46
6518.37	2.830	-2.450	56.2	7.36
6581.21	1.480	-4.680	20.8	7.51
6591.33	4.593	-1.950	10.4	7.44
6608.04	2.279	-3.914	17.2	7.43
6699.14	4.590	-2.100	7.9	7.45
6703.57	2.759	-3.023	36.1	7.46
6705.10	4.607	-0.980	45.4	7.38
6713.75	4.795	-1.400	20.8	7.44
6725.36	4.103	-2.167	17.0	7.44
6726.67	4.607	-1.030	46.0	7.43
6733.15	4.638	-1.400	25.9	7.43
6739.52	1.560	-4.794	11.5	7.39
6793.26	4.076	-2.326	12.4	7.41
6810.26	4.607	-0.986	48.6	7.44
6828.59	4.640	-0.820	54.6	7.41
6837.01	4.590	-1.687	17.6	7.44
6842.69	4.640	-1.220	39.1	7.52
6843.66	4.550	-0.830	59.5	7.42
6857.25	4.076	-2.038	22.3	7.43
6971.94	3.020	-3.340	12.6	7.41

Table 1 – continued from previous page

Wavelength Å	LEP eV	$\log gf$	$W_{\lambda_{\odot}}$ mÅ	$\log \varepsilon_{\odot}$ dex
6999.88	4.100	-1.460	53.8	7.52
7022.95	4.190	-1.150	63.6	7.47
7132.99	4.080	-1.650	42.1	7.47
7751.12	4.990	-0.730	45.3	7.43
7802.51	5.080	-1.310	15.4	7.41
7807.92	4.990	-0.509	58.8	7.44
Fe II				
5234.62	3.221	-2.180	83.3	7.36
5264.80	3.230	-3.130	47.9	7.53
5414.07	3.221	-3.580	27.5	7.50
5425.26	3.200	-3.220	41.3	7.44
6149.25	3.889	-2.630	35.7	7.36
6247.56	3.892	-2.271	52.8	7.39
6369.46	2.891	-4.110	19.4	7.48
6432.68	2.891	-3.570	40.9	7.46
6456.39	3.903	-2.065	62.3	7.39
6516.08	2.891	-3.310	52.6	7.45

Table 2: Derived Atmospheric Parameters of giants from the Hercules stream.
Columns are self explanatory.

Star	$(T_{\text{eff}})_{J-K}$ K	$(T_{\text{eff}})_{V-K}$ K	$(T_{\text{eff}})_{\text{spec}}$ K	$\log g$ (phot) cm s^{-2}	$\log g$ (spec) cm s^{-2}	ξ_t km s^{-1}	[M/H] dex	Age Gyr
HIP 258	4304	4953	4770	2.61 ± 0.05	2.98	1.46	+0.27	0.7 ± 0.2
HIP 504	4833	4811	4830	2.65 ± 0.08	2.80	1.50	+0.17	0.8 ± 0.3
HIP 3546	4617	4572	4640	2.52 ± 0.12	2.58	1.55	+0.25	1.5 ± 1.3
HIP 3719	4752	4706	4840	2.60 ± 0.09	2.76	1.53	+0.04	0.9 ± 0.4
HIP 4486	4138	4649	4770	2.96 ± 0.07	3.08	1.25	+0.17	3.4 ± 1.0
HIP 6682	4858	4886	4920	3.18 ± 0.07	3.32	1.22	+0.16	2.5 ± 0.7
HIP 7119	4699	4806	4960	2.78 ± 0.22	3.00	1.46	+0.09	1.0 ± 0.6
HIP 7710	4486	4580	4650	2.43 ± 0.07	2.65	1.35	-0.11	6.1 ± 2.8
HIP 8926	4918	4997	5100	3.02 ± 0.11	3.16	1.44	+0.23	0.8 ± 0.2
HIP 8984	4975	4656	4800	2.71 ± 0.12	2.70	1.47	+0.05	1.8 ± 0.7
HIP 9307	4896	5019	4920	2.64 ± 0.04	2.85	1.51	+0.01	0.7 ± 0.2
HIP 9517	4940	4799	4800	2.58 ± 0.11	2.62	1.46	-0.01	2.4 ± 1.3
HIP 11117	4575	4757	4820	3.19 ± 0.08	3.34	1.23	+0.38	2.8 ± 0.9
HIP 13786	4306	4693	4650	2.52 ± 0.13	2.60	1.62	+0.15	3.9 ± 2.5
HIP 18865	4737	4555	4960	3.05 ± 0.25	3.10	1.42	+0.30	1.4 ± 0.6
HIP 19287	4552	4501	4690	2.72 ± 0.10	2.65	1.54	+0.24	1.8 ± 0.6
HIP 20540	4797	5078	4965	2.84 ± 0.06	3.20	1.26	+0.03	1.3 ± 0.2
HIP 20771	4346	4966	4870	2.78 ± 0.05	3.00	1.42	+0.31	1.2 ± 0.3
HIP 22176	4460	4489	4660	2.71 ± 0.08	2.90	1.51	+0.30	1.7 ± 0.6
HIP 22661	4488	4389	4630	2.58 ± 0.10	2.77	1.70	+0.32	1.8 ± 1.1
HIP 22765	4631	4710	4730	2.62 ± 0.09	2.75	1.59	+0.20	1.3 ± 0.7
HIP 28168	4455	4511	4670	2.87 ± 0.08	3.15	1.37	+0.40	2.5 ± 0.8
HIP 28417	4770	4758	4900	2.68 ± 0.12	2.75	1.51	-0.09	1.7 ± 0.7
HIP 28677	5323	4981	4910	3.04 ± 0.09	3.10	1.30	-0.06	3.6 ± 1.0
HIP 29949	4510	4540	4710	2.55 ± 0.09	2.70	1.53	+0.14	2.7 ± 1.3
HIP 31039	5035	5170	5030	3.15 ± 0.06	3.35	1.25	-0.05	2.1 ± 0.5
HIP 32261	4965	4747	4850	3.05 ± 0.05	3.23	1.26	+0.32	1.3 ± 0.2
HIP 32844	4561	4329	4480	2.12 ± 0.07	2.34	1.61	+0.17	0.7 ± 0.2
HIP 35146	4392	4747	4790	2.80 ± 0.04	3.06	1.29	+0.26	1.4 ± 0.2
HIP 36647	4766	4649	4680	2.66 ± 0.14	2.65	1.45	+0.10	3.5 ± 1.7
HIP 37049	4895	4820	4930	2.77 ± 0.07	3.00	1.48	+0.10	1.1 ± 0.3
HIP 37441	4683	4745	4930	2.62 ± 0.11	2.75	1.62	-0.16	1.7 ± 0.9
HIP 48140	4489	4549	4680	2.60 ± 0.10	2.65	1.46	+0.27	1.4 ± 0.8
HIP 48417	4493	4324	4440	2.44 ± 0.11	2.33	1.41	+0.05	7.1 ± 2.6
HIP 50526	4567	4820	4870	2.71 ± 0.08	2.78	1.52	+0.06	1.2 ± 0.5
HIP 51047	4716	4673	4830	2.76 ± 0.07	2.80	1.52	+0.12	1.4 ± 0.4
HIP 52882	4780	4726	4670	2.29 ± 0.08	2.58	1.51	-0.02	0.9 ± 0.4
HIP 58654	4854	4564	4840	2.61 ± 0.09	2.64	1.47	-0.02	1.4 ± 0.7
HIP 87629	5113	5013	5090	3.26 ± 0.08	3.42	1.27	+0.08	1.6 ± 0.3
HIP 94576	4949	4884	5050	2.92 ± 0.08	3.20	1.45	+0.28	0.8 ± 0.2
HIP 95375	4736	4786	4760	2.83 ± 0.06	3.00	1.31	+0.15	1.8 ± 0.6
HIP 96028	4535	4581	4700	2.76 ± 0.07	2.93	1.29	+0.16	2.2 ± 0.9
HIP 96294	4601	4823	4880	2.65 ± 0.09	3.00	1.48	+0.30	0.7 ± 0.2
HIP 102010	4376	4720	4710	2.51 ± 0.14	2.70	1.56	+0.13	1.4 ± 1.3
HIP 104035	4871	4966	5040	2.85 ± 0.09	3.05	1.42	+0.20	1.0 ± 0.2
HIP 105502	4820	5021	4770	2.62 ± 0.04	2.86	1.55	+0.17	0.8 ± 0.2
HIP 106551	4464	4901	4840	2.68 ± 0.04	2.88	1.59	+0.18	0.9 ± 0.2
HIP 107502	4380	4865	4610	2.51 ± 0.08	2.75	1.38	+0.25	2.9 ± 1.5
HIP 108012	4348	4459	4580	2.43 ± 0.08	2.65	1.44	+0.14	3.4 ± 1.9
HIP 108914	4806	4785	4860	2.79 ± 0.05	3.15	1.44	+0.42	1.2 ± 0.3
HIP 109387	4864	5011	5000	3.20 ± 0.06	3.40	1.27	+0.20	1.5 ± 0.3
HIP 109585	4233	5249	4760	2.65 ± 0.05	2.72	1.52	+0.18	1.0 ± 0.3
HIP 111728	4407	4569	4610	2.69 ± 0.10	2.94	1.47	+0.33	2.4 ± 1.1
HIP 113144	4735	4762	4980	3.23 ± 0.07	3.40	1.19	+0.10	2.3 ± 0.6
HIP 114742	4750	2.49 ± 0.06	2.93	1.63	+0.35	0.5 ± 0.1
HIP 115899	5091	4840	4910	2.70 ± 0.06	2.95	1.44	+0.12	0.9 ± 0.3
HIP 116348	4714	4833	4830	2.72 ± 0.09	2.77	1.53	+0.10	1.4 ± 0.5
HIP 116644	4605	4553	4760	2.60 ± 0.15	2.88	1.45	+0.13	1.2 ± 0.9

Table 3: Adopted line list for elements other than Iron

Species	Wavelength Å	LEP eV	$\log gf$	$W_{\lambda_{\odot}}$ mÅ	$\log \varepsilon_{\odot}$ dex
Na I	6154.23	2.10	-1.55	36.6	6.28
	6160.75	2.10	-1.25	56.5	6.29
Mg I	5711.09	4.34	-1.73	104.1	7.54
	6318.72	5.11	-1.95	44.5	7.58
	6319.24	5.11	-2.32	27.4	7.65
	7657.61	5.11	-1.28	98.5	7.59
Al I	6696.02	3.14	-1.48	36.9	6.40
	6698.67	3.14	-1.78	20.8	6.36
	7835.31	4.02	-0.69	41.1	6.41
	7836.13	4.02	-0.45	55.0	6.36
Si I	5690.42	4.93	-1.77	48.1	7.47
	5701.10	4.93	-1.95	37.9	7.47
	5772.15	5.08	-1.65	52.3	7.55
	6142.49	5.62	-1.540	33.3	7.58
Ca I	6145.02	5.61	-1.479	37.6	7.59
	5260.39	2.52	-1.72	32.1	6.27
	5867.56	2.93	-1.57	22.6	6.27
	6166.44	2.52	-1.14	69.1	6.31
	6169.04	2.52	-0.80	90.3	6.32
	6169.56	2.53	-0.48	108.7	6.28
	6455.60	2.52	-1.34	55.9	6.28
	6471.66	2.53	-0.69	90.6	6.20
Sc II	6499.65	2.52	-0.82	84.7	6.23
	5357.20	1.51	-2.11	4.8	3.19
	5552.23	1.46	-2.28	4.6	3.28
	5684.21	1.51	-1.07	37.1	3.24
	6245.64	1.51	-1.04	35.2	3.14
	6300.75	1.51	-1.95	8.2	3.24
Ti I	6320.84	1.50	-1.92	8.9	3.24
	5295.77	1.07	-1.58	13.2	4.95
	5490.15	1.46	-0.88	22.0	4.89
	5702.66	2.29	-0.59	7.3	4.83
	5716.44	2.30	-0.72	5.9	4.87
	6092.79	1.89	-1.32	4.1	4.89
	6303.75	1.44	-1.51	8.8	4.99
	6312.23	1.46	-1.50	8.1	4.95
	6599.10	0.90	-2.03	9.3	4.98
	7357.73	1.44	-1.07	22.2	4.97
Ti II	4583.41	1.17	-2.87	33.0	5.06
	4708.66	1.24	-2.37	53.3	5.04
	5336.78	1.58	-1.63	71.7	4.96
	5418.77	1.58	-2.11	48.5	4.97
V I	6039.73	1.06	-0.65	12.3	3.93
	6081.44	1.05	-0.58	13.0	3.87
	6090.21	1.08	-0.06	32.3	3.89
	6119.53	1.06	-0.32	21.0	3.88
	6135.36	1.05	-0.75	10.2	3.91
	6274.65	0.27	-1.67	6.9	3.87
Cr I	5287.20	3.44	-0.89	11.3	5.65
	5300.74	0.98	-2.08	59.3	5.60
	5304.18	3.46	-0.68	16.0	5.63
	5628.62	3.42	-0.76	14.7	5.62
	5781.16	3.01	-1.00	16.7	5.54
	6882.48	3.44	-0.38	32.4	5.67
Mn I	6883.00	3.44	-0.42	30.5	5.67
	4671.69	2.89	-1.66	14.8	5.47

Table 3 – continued from previous page

Species	Wavelength Å	LEP eV	logg <i>f</i>	$W_{\lambda_{\odot}}$ mÅ	log ε_{\odot} dex
Co I	4739.11	2.94	-0.60	60.7	5.39
	5004.89	2.92	-1.64	14.0	5.45
	5280.63	3.63	-0.03	20.3	4.90
	5352.04	3.58	0.06	25.1	4.88
	5647.23	2.28	-1.56	13.9	4.90
Ni I	6455.00	3.63	-0.25	14.8	4.89
	5088.96	3.678	-1.240	28.2	6.19
	5094.42	3.833	-1.074	30.4	6.22
	5115.40	3.834	-0.281	75.2	6.29
	6111.08	4.088	-0.808	33.6	6.22
	6130.14	4.266	-0.938	21.6	6.24
	6175.37	4.089	-0.550	47.7	6.24
	6176.80	4.09	-0.26	62.0	6.22
	6177.25	1.826	-3.508	14.1	6.22
	6772.32	3.658	-0.972	48.0	6.24
	7797.59	3.900	-0.348	75.3	6.27
	7826.77	3.700	-1.840	12.5	6.23
Zn I	4810.54	4.080	-0.170	71.6	4.45
Ba II	6362.35	5.790	0.140	21.2	4.53
	5853.68	0.604	-1.000	60.3	2.15
	6141.73	0.704	-0.032	109.1	2.23

Table 4. Derived solar abundances compared with the values of Asplund et al. (2009). σ is the standard deviation or line to line scatter and N is the number of lines used

Species	($\log \varepsilon \pm \sigma$) dex (Current)	N	($\log \varepsilon \pm \sigma$) dex (Asplund)	Difference dex
Na I	6.29 ± 0.01	2	6.24 ± 0.04	+0.05
Mg I	7.59 ± 0.04	4	7.60 ± 0.04	−0.01
Al I	6.38 ± 0.03	4	6.45 ± 0.03	−0.07
Si I	7.53 ± 0.06	5	7.51 ± 0.03	+0.02
Ca I	6.27 ± 0.04	8	6.34 ± 0.04	−0.07
Sc II	3.21 ± 0.05	6	3.15 ± 0.04	+0.06
Ti I	4.93 ± 0.06	9	4.95 ± 0.05	−0.02
Ti II	5.01 ± 0.05	4	4.95 ± 0.05	+0.06
V I	3.89 ± 0.03	6	3.93 ± 0.08	−0.04
Cr I	5.63 ± 0.05	7	5.64 ± 0.04	−0.01
Mn I	5.44 ± 0.04	3	5.43 ± 0.04	+0.01
Fe I	7.44 ± 0.05	60	7.50 ± 0.04	−0.06
Fe II	7.44 ± 0.06	10	7.50 ± 0.04	−0.06
Co I	4.85 ± 0.02	4	4.99 ± 0.07	−0.14
Ni I	6.23 ± 0.03	11	6.22 ± 0.04	+0.01
Zn I	4.49 ± 0.05	1	4.56 ± 0.05	−0.06
Ba II	2.10 ± 0.02	2	2.18 ± 0.09	−0.08

Table 5: The elemental abundances for Hercules stream members for the elements Na, Mg, Al, Si, Ca and Sc given as [El/Fe]. σ is the standard deviation or line to line scatter where N is the number of lines. Hyperfine corrections are applied for Sc. Mean of [FeI/H] and [FeII/H] is used as [Fe/H] throughout

Star	[FeI/H] σ N	[FeII/H] σ N	[Na/Fe] σ N	[Mg/Fe] σ N	[Al/Fe] σ N	[Si/Fe] σ N	[Ca/Fe] σ N	[Sc/Fe] σ N
HIP 258	+0.26 0.08 56	+0.27 0.05 8	0.25 0.01 2	-0.04 0.04 4	0.18 0.06 4	0.09 0.06 5	-0.05 0.06 8	0.06 0.04 6
HIP 504	+0.17 0.07 57	+0.16 0.03 8	0.09 0.04 2	0.02 0.03 4	0.12 0.05 4	0.06 0.06 5	0.03 0.06 8	-0.03 0.05 6
HIP 3546	+0.24 0.07 55	+0.24 0.06 8	0.27 0.02 2	0.00 0.04 4	0.13 0.03 4	0.11 0.07 5	-0.03 0.07 8	-0.06 0.05 6
HIP 3719	+0.04 0.06 57	+0.03 0.06 8	0.07 0.01 2	0.07 0.02 3	0.12 0.06 4	0.08 0.06 5	0.06 0.04 8	0.04 0.03 6
HIP 4486	+0.16 0.08 56	+0.15 0.06 8	0.09 0.03 2	0.01 0.03 4	0.16 0.07 4	0.07 0.07 5	0.02 0.05 8	0.06 0.02 6
HIP 6682	+0.13 0.06 57	+0.15 0.04 8	0.00 0.02 2	-0.02 0.01 4	0.06 0.02 4	0.03 0.05 5	0.01 0.07 8	0.03 0.05 6
HIP 7119	+0.07 0.06 57	+0.07 0.05 8	0.09 0.01 2	-0.01 0.06 4	0.03 0.03 4	0.05 0.06 5	0.05 0.05 8	0.03 0.04 6
HIP 7710	-0.13 0.06 57	-0.13 0.05 8	0.03 0.05 2	0.11 0.03 4	0.21 0.04 4	0.12 0.06 5	0.08 0.04 8	0.06 0.02 6
HIP 8926	+0.22 0.06 57	+0.21 0.04 8	0.16 0.02 2	-0.06 0.02 4	0.04 0.04 4	0.04 0.06 5	0.06 0.05 8	-0.03 0.03 6
HIP 8984	+0.04 0.06 57	+0.03 0.03 8	0.07 0.03 2	0.05 0.01 4	0.13 0.03 4	0.10 0.06 5	0.03 0.05 8	0.04 0.05 6
HIP 9307	+0.01 0.06 56	+0.01 0.03 8	0.07 0.03 2	0.04 0.05 4	0.12 0.06 4	0.05 0.06 5	0.05 0.05 8	0.04 0.05 6
HIP 9517	+0.00 0.06 57	-0.02 0.07 8	0.02 0.03 2	0.05 0.05 3	0.23 0.07 4	0.07 0.05 5	0.10 0.04 8	-0.10 0.05 4
HIP 11117	+0.38 0.08 56	+0.37 0.07 8	0.22 0.02 2	0.04 0.05 4	0.17 0.04 4	0.05 0.06 5	-0.05 0.07 8	0.03 0.04 6
HIP 13786	+0.13 0.08 55	+0.14 0.07 9	0.24 0.06 2	-0.06 0.07 4	0.30 0.03 4	0.09 0.07 5	0.04 0.06 8	0.02 0.09 6
HIP 18865	+0.33 0.07 56	+0.33 0.07 8	0.29 0.01 2	-0.03 0.01 2	0.06 0.05 4	0.08 0.07 5	0.02 0.05 8	0.02 0.08 6
HIP 19287	+0.24 0.07 57	+0.22 0.07 8	0.17 0.00 2	0.01 0.03 4	0.12 0.03 4	0.06 0.07 5	0.00 0.07 8	-0.03 0.04 4
HIP 20540	+0.03 0.06 57	+0.03 0.05 8	0.12 0.02 2	0.00 0.03 3	0.09 0.02 4	0.04 0.06 5	0.07 0.04 8	0.02 0.05 4
HIP 20771	+0.29 0.07 57	+0.30 0.06 8	0.17 0.00 2	-0.12 0.05 3	0.06 0.05 4	0.03 0.05 5	-0.01 0.05 8	-0.04 0.05 6
HIP 22176	+0.32 0.07 55	+0.31 0.07 8	0.40 0.03 2	-0.05 0.03 3	0.14 0.02 4	0.06 0.06 5	-0.02 0.07 8	0.07 0.04 5
HIP 22661	+0.31 0.08 55	+0.33 0.08 8	0.38 0.04 2	0.04 0.07 4	0.20 0.05 4	0.14 0.07 5	-0.12 0.08 7	0.03 0.04 6
HIP 22765	+0.19 0.08 56	+0.20 0.08 8	0.15 0.01 2	-0.05 0.08 4	0.12 0.02 4	0.10 0.06 5	-0.03 0.07 8	-0.05 0.04 6
HIP 28168	+0.42 0.08 57	+0.44 0.08 8	0.18 0.01 2	-0.07 0.06 4	0.13 0.07 4	0.02 0.07 5	-0.11 0.07 8	0.08 0.05 6
HIP 28417	-0.10 0.06 57	-0.11 0.05 8	0.02 0.02 2	0.11 0.05 3	0.16 0.05 4	0.10 0.08 5	0.08 0.04 8	0.09 0.05 4
HIP 28677	-0.08 0.05 57	-0.08 0.05 9	0.05 0.02 2	0.07 0.06 4	0.15 0.05 4	0.06 0.05 5	0.07 0.03 8	-0.01 0.04 6
HIP 29949	+0.13 0.07 57	+0.12 0.06 8	0.17 0.00 2	0.17 0.04 3	0.22 0.03 4	0.12 0.07 5	0.05 0.07 8	0.02 0.05 6
HIP 31039	-0.03 0.06 57	-0.03 0.04 8	0.04 0.04 2	0.00 0.05 3	0.08 0.02 4	0.05 0.05 5	0.06 0.03 8	-0.02 0.06 6
HIP 32261	+0.31 0.08 57	+0.30 0.05 8	0.25 0.01 2	-0.01 0.02 4	0.15 0.06 4	0.06 0.06 5	-0.02 0.06 8	0.05 0.05 6
HIP 32844	+0.17 0.07 57	+0.19 0.05 8	0.10 0.01 2	-0.04 0.05 4	0.12 0.05 4	0.10 0.07 5	-0.10 0.06 8	0.01 0.03 5
HIP 35146	+0.27 0.07 57	+0.28 0.06 8	0.06 0.04 2	-0.04 0.06 4	0.08 0.06 4	0.02 0.06 5	-0.06 0.06 8	-0.04 0.04 6
HIP 36647	+0.11 0.08 58	+0.11 0.07 8	0.08 0.00 2	0.13 0.05 4	0.15 0.03 4	0.12 0.07 5	0.00 0.06 8	0.01 0.07 5
HIP 37049	+0.09 0.05 57	+0.09 0.04 8	0.11 0.02 2	-0.04 0.07 3	0.09 0.03 4	0.05 0.06 5	0.02 0.05 8	0.03 0.04 6
HIP 37441	-0.16 0.05 57	-0.17 0.03 8	0.10 0.04 2	0.07 0.07 3	0.14 0.03 4	0.11 0.06 5	0.09 0.04 8	0.09 0.04 6
HIP 48140	+0.29 0.07 56	+0.31 0.05 8	0.21 0.00 2	0.01 0.07 4	0.12 0.07 4	0.02 0.05 5	-0.08 0.07 8	-0.07 0.05 6
HIP 48417	+0.03 0.07 57	+0.05 0.07 8	0.12 0.00 2	0.05 0.05 3	0.19 0.06 4	0.09 0.03 5	-0.01 0.05 8	0.03 0.06 5
HIP 50526	+0.06 0.06 57	+0.05 0.04 8	0.08 0.02 2	0.01 0.03 4	0.11 0.04 4	0.09 0.06 5	0.05 0.05 8	-0.03 0.05 6
HIP 51047	+0.12 0.06 57	+0.10 0.05 8	0.12 0.03 2	0.02 0.07 4	0.15 0.06 4	0.05 0.06 5	0.03 0.05 8	0.00 0.05 6

Table 5 – continued from previous page

Star	[FeI/H] σ N	[FeII/H] σ N	[Na/Fe] σ N	[Mg/Fe] σ N	[Al/Fe] σ N	[Si/Fe] σ N	[Ca/Fe] σ N	[Sc/Fe] σ N
HIP 52882	-0.02 0.06 57	-0.04 0.06 8	0.17 0.04 2	0.03 0.06 4	0.11 0.02 4	0.06 0.05 5	0.02 0.05 8	0.06 0.05 6
HIP 58654	-0.01 0.06 57	-0.03 0.03 9	0.10 0.03 2	0.07 0.02 4	0.18 0.03 4	0.07 0.05 5	0.09 0.06 8	0.00 0.04 6
HIP 87629	+0.06 0.05 56	+0.05 0.07 8	-0.02 0.02 2	-0.02 0.07 2	0.01 0.03 4	0.03 0.06 5	0.05 0.05 8	0.02 0.09 5
HIP 94576	+0.27 0.07 54	+0.26 0.06 8	0.44 0.01 2	0.10 0.08 2	0.21 0.06 4	0.03 0.07 5	0.06 0.06 8	0.04 0.07 6
HIP 95375	+0.14 0.06 56	+0.12 0.06 8	0.09 0.03 2	0.06 0.07 2	0.08 0.04 4	0.06 0.07 5	-0.02 0.06 8	0.02 0.07 6
HIP 96028	+0.16 0.07 55	+0.18 0.06 8	0.05 0.04 2	0.00 0.02 3	0.10 0.04 4	0.06 0.04 5	-0.01 0.05 8	0.04 0.06 6
HIP 96294	+0.29 0.07 55	+0.27 0.07 8	0.23 0.01 2	-0.06 0.02 3	0.06 0.03 4	0.02 0.07 5	0.00 0.07 8	0.06 0.07 6
HIP 102010	+0.12 0.07 57	+0.11 0.05 7	0.11 0.05 2	0.18 0.04 3	0.20 0.05 4	0.13 0.06 5	-0.01 0.08 8	0.07 0.06 6
HIP 104035	+0.18 0.06 56	+0.16 0.03 8	0.07 0.03 2	-0.02 0.05 3	0.00 0.02 4	0.02 0.06 5	0.08 0.06 8	-0.03 0.06 6
HIP 105502	+0.18 0.06 56	+0.18 0.06 7	-0.01 0.09 2	0.03 0.05 2	0.13 0.07 4	0.06 0.05 5	-0.03 0.08 8	0.09 0.06 4
HIP 106551	+0.18 0.08 56	+0.19 0.06 8	0.17 0.01 2	-0.08 0.02 2	0.11 0.07 4	0.06 0.05 5	-0.04 0.07 8	0.07 0.08 5
HIP 107502	+0.23 0.06 57	+0.23 0.05 8	0.11 0.03 2	0.06 0.02 3	0.12 0.06 4	0.06 0.07 5	-0.02 0.06 8	0.02 0.01 6
HIP 108012	+0.16 0.07 56	+0.15 0.07 8	0.20 0.02 2	0.08 0.06 3	0.12 0.05 4	0.10 0.06 5	-0.01 0.07 8	0.01 0.04 6
HIP 108914	+0.43 0.08 55	+0.42 0.06 8	0.29 0.05 2	-0.08 0.05 2	0.14 0.06 4	0.07 0.06 5	-0.06 0.07 8	0.08 0.06 6
HIP 109387	+0.21 0.07 56	+0.21 0.06 9	0.07 0.01 2	0.06 0.06 4	0.07 0.03 4	0.03 0.04 5	-0.04 0.05 8	-0.01 0.05 6
HIP 109585	+0.21 0.07 55	+0.19 0.04 8	0.15 0.04 2	0.10 0.06 4	0.14 0.04 4	0.07 0.05 5	0.01 0.08 8	0.01 0.05 6
HIP 111728	+0.31 0.08 55	+0.32 0.06 8	0.34 0.03 2	0.07 0.04 3	0.22 0.04 4	0.10 0.03 5	-0.06 0.07 8	0.08 0.05 6
HIP 113144	+0.09 0.07 55	+0.10 0.05 8	-0.01 0.02 2	0.05 0.10 3	0.09 0.06 4	0.03 0.04 5	0.04 0.05 8	0.09 0.05 5
HIP 114742	+0.36 0.07 55	+0.37 0.07 8	0.33 0.03 2	0.04 0.05 4	0.21 0.06 4	0.13 0.08 5	-0.06 0.08 8	0.10 0.05 6
HIP 115899	+0.09 0.06 56	+0.11 0.05 8	0.04 0.05 2	0.01 0.03 3	0.03 0.03 4	0.06 0.06 5	0.04 0.04 8	0.05 0.06 6
HIP 116348	+0.08 0.06 57	+0.08 0.05 8	0.06 0.02 2	0.03 0.05 4	0.15 0.04 4	0.08 0.06 5	0.03 0.05 8	0.02 0.04 6
HIP 116644	+0.13 0.07 56	+0.15 0.05 8	0.09 0.02 2	-0.01 0.08 4	0.00 0.02 4	0.07 0.02 5	-0.05 0.05 8	0.02 0.05 6

Table 6: The elemental abundances for Hercules stream members for the elements Ti, V, Cr, Mn, Co, Ni, Zn and Ba given as [El/Fe]. σ is the standard deviation or line to line scatter where N is the number of lines. Hyperfine correction are applied for V, Mn, Co and Ba

Star	[TiI/Fe] σ N	[TiII/Fe] σ N	[V/Fe] σ N	[Cr/Fe] σ N	[Mn/Fe] σ N	[Co/Fe] σ N	[Ni/Fe] σ N	[Zn/Fe] σ N	[Ba/Fe] σ N
HIP 258	-0.05 0.08 8	-0.01 0.04 4	-0.03 0.05 5	0.02 0.06 6	0.03 0.06 3	0.07 0.07 4	0.11 0.06 11	0.14 0.26 2	0.02 0.02 2
HIP 504	-0.05 0.04 7	-0.01 0.02 4	-0.01 0.05 5	-0.01 0.05 5	-0.03 0.06 3	0.03 0.06 4	0.05 0.05 11	0.05 0.18 2	0.18 0.04 2
HIP 3546	-0.09 0.07 8	-0.15 0.04 4	-0.06 0.07 5	0.01 0.06 6	-0.09 0.05 3	0.05 0.06 4	0.10 0.06 11	0.17 0.35 2	0.01 0.04 2
HIP 3719	0.01 0.06 8	0.05 0.03 4	0.01 0.03 5	-0.01 0.04 6	-0.10 0.03 3	-0.02 0.07 4	0.03 0.05 11	0.03 0.10 2	0.29 0.07 2
HIP 4486	0.02 0.07 8	0.07 0.01 4	0.04 0.07 5	0.01 0.06 5	-0.02 0.03 3	0.03 0.06 4	0.08 0.05 11	0.09 0.22 2	0.15 0.08 2
HIP 6682	0.00 0.07 8	0.06 0.04 4	0.03 0.03 5	0.00 0.05 6	-0.06 0.04 3	-0.02 0.05 4	0.03 0.07 11	0.02 0.09 2	0.19 0.06 2
HIP 7119	-0.01 0.06 8	0.06 0.07 4	0.03 0.04 5	0.00 0.04 5	-0.06 0.02 3	-0.03 0.05 4	0.01 0.05 11	0.00 0.06 2	0.31 0.06 2
HIP 7710	0.07 0.06 8	0.10 0.03 4	0.02 0.03 5	0.01 0.04 6	-0.08 0.03 3	0.01 0.06 4	0.04 0.06 11	0.08 0.15 2	0.13 0.06 2
HIP 8926	0.01 0.07 8	0.01 0.05 4	0.01 0.03 5	-0.01 0.05 6	-0.07 0.01 3	-0.05 0.05 4	0.02 0.04 11	-0.05 0.07 2	0.26 0.02 2
HIP 8984	-0.03 0.05 8	0.07 0.06 4	0.01 0.04 5	-0.01 0.05 6	-0.11 0.03 3	0.02 0.05 4	0.05 0.06 11	0.09 0.13 2	0.19 0.05 2
HIP 9307	0.03 0.07 8	0.07 0.06 4	0.06 0.04 5	-0.01 0.06 6	-0.05 0.04 3	0.00 0.06 4	0.02 0.05 10	0.06 0.05 2	0.23 0.06 2
HIP 9517	0.14 0.05 8	0.07 0.09 4	0.08 0.03 5	0.06 0.07 4	-0.13 0.05 2	-0.05 0.05 4	0.01 0.07 11	-0.11 0.00 1	0.28 0.05 2
HIP 11117	-0.03 0.07 8	-0.06 0.03 4	0.02 0.05 5	-0.01 0.05 6	-0.03 0.05 3	0.05 0.05 4	0.13 0.06 11	0.18 0.28 2	-0.01 0.03 2
HIP 13786	0.10 0.05 8	-0.08 0.05 4	0.11 0.04 5	0.08 0.02 6	-0.13 0.07 3	0.08 0.04 4	0.07 0.04 11	0.08 0.19 2	0.12 0.07 2
HIP 18865	-0.03 0.05 8	-0.06 0.05 4	0.04 0.05 5	0.04 0.06 5	-0.04 0.06 3	0.01 0.06 4	0.10 0.04 11	0.13 0.12 2	-0.03 0.02 2
HIP 19287	-0.01 0.05 8	-0.08 0.03 4	-0.01 0.06 5	0.01 0.06 5	-0.09 0.03 3	0.05 0.06 4	0.08 0.04 11	0.13 0.23 2	0.06 0.03 2
HIP 20540	0.01 0.04 7	0.01 0.04 4	0.05 0.03 5	0.00 0.06 5	-0.08 0.02 3	-0.02 0.05 4	0.03 0.05 11	0.05 0.14 2	0.20 0.02 2
HIP 20771	-0.07 0.07 7	0.01 0.03 4	-0.03 0.03 5	0.01 0.06 5	-0.06 0.03 3	-0.03 0.05 4	0.05 0.05 10	0.05 0.11 2	0.17 0.06 2
HIP 22176	0.02 0.08 8	-0.10 0.05 4	0.11 0.06 5	0.06 0.07 6	-0.05 0.03 3	0.08 0.08 4	0.11 0.07 11	0.13 0.29 2	-0.01 0.05 2
HIP 22661	0.01 0.08 8	-0.11 0.06 4	0.08 0.04 5	0.01 0.06 5	-0.06 0.05 3	0.16 0.06 4	0.14 0.07 11	0.24 0.48 2	-0.09 0.01 2
HIP 22765	-0.06 0.05 8	-0.05 0.03 4	-0.03 0.05 5	-0.02 0.06 6	-0.04 0.04 3	0.06 0.05 4	0.08 0.04 11	0.14 0.26 2	0.09 0.04 2
HIP 28168	-0.02 0.07 8	-0.06 0.05 4	0.05 0.06 5	-0.01 0.06 5	-0.02 0.04 3	0.04 0.08 4	0.08 0.06 11	0.15 0.37 2	0.01 0.07 2
HIP 28417	0.04 0.06 7	0.11 0.06 4	0.08 0.02 4	-0.03 0.05 6	-0.09 0.05 3	0.03 0.04 4	0.04 0.05 11	0.14 0.10 2	0.16 0.04 2
HIP 28677	0.06 0.07 8	0.05 0.03 4	0.07 0.03 5	0.00 0.06 5	-0.07 0.01 3	0.01 0.05 4	0.03 0.06 11	0.06 0.15 2	0.09 0.02 2
HIP 29949	0.07 0.05 8	0.03 0.02 4	0.08 0.05 5	0.03 0.04 6	-0.08 0.05 3	0.11 0.05 4	0.08 0.05 11	0.20 0.16 2	0.13 0.07 2
HIP 31039	0.01 0.08 8	0.04 0.01 4	0.02 0.03 5	0.00 0.06 5	-0.09 0.02 3	-0.04 0.05 4	0.02 0.06 11	0.08 0.10 2	0.16 0.03 2
HIP 32261	-0.01 0.06 8	0.01 0.03 4	0.01 0.05 5	0.03 0.06 6	-0.02 0.01 3	0.05 0.05 4	0.12 0.05 11	0.09 0.19 2	0.11 0.07 2
HIP 32844	-0.12 0.07 8	-0.02 0.06 4	-0.06 0.06 5	-0.02 0.07 6	-0.08 0.08 3	-0.03 0.07 4	0.03 0.07 11	0.08 0.29 2	0.19 0.06 2
HIP 35146	-0.12 0.06 7	-0.08 0.02 4	-0.08 0.06 5	-0.09 0.04 4	-0.07 0.04 3	-0.07 0.04 4	0.04 0.08 12	0.03 0.13 2	0.18 0.06 2
HIP 36647	0.01 0.05 8	0.06 0.04 4	-0.01 0.04 5	-0.06 0.04 4	-0.18 0.06 3	0.03 0.05 4	0.04 0.06 11	0.24 0.11 2	0.13 0.07 2
HIP 37049	-0.01 0.06 8	0.09 0.05 4	0.01 0.04 5	-0.02 0.06 5	-0.07 0.03 3	0.01 0.06 4	0.03 0.04 11	0.05 0.15 2	0.21 0.05 2
HIP 37441	0.06 0.06 8	0.08 0.04 4	0.10 0.03 5	-0.01 0.06 5	-0.07 0.02 3	0.05 0.04 4	0.01 0.03 11	0.02 0.08 2	0.27 0.03 2
HIP 48140	-0.11 0.08 8	-0.01 0.03 4	-0.10 0.04 5	-0.07 0.05 5	-0.09 0.04 3	0.00 0.05 4	0.03 0.07 10	0.08 0.18 2	0.10 0.07 2
HIP 48417	-0.04 0.05 8	-0.05 0.02 4	-0.01 0.06 5	-0.06 0.04 4	-0.05 0.04 3	-0.01 0.05 4	0.06 0.05 9	0.14 0.30 2	0.09 0.06 2
HIP 50526	0.01 0.06 8	0.06 0.05 4	-0.01 0.06 5	-0.01 0.06 6	-0.05 0.04 2	-0.02 0.06 4	0.04 0.05 11	0.03 0.15 2	0.17 0.03 2
HIP 51047	-0.01 0.06 8	0.03 0.04 4	0.03 0.04 5	0.03 0.05 6	-0.04 0.02 3	0.04 0.05 4	0.08 0.04 11	0.08 0.17 2	0.18 0.03 2
HIP 52882	0.03 0.07 8	0.06 0.04 4	0.04 0.04 5	-0.01 0.04 6	-0.08 0.05 3	0.03 0.05 4	0.03 0.04 11	0.09 0.26 2	0.20 0.05 2

Table 6 – continued from previous page

Star	[TiI/Fe] σ N	[TiII/Fe] σ N	[V/Fe] σ N	[Cr/Fe] σ N	[Mn/Fe] σ N	[Co/Fe] σ N	[Ni/Fe] σ N	[Zn/Fe] σ N	[Ba/Fe] σ N
HIP 58654	0.03 0.06 8	0.00 0.05 4	0.08 0.04 5	0.03 0.05 6	-0.07 0.04 3	0.01 0.05 4	0.03 0.05 11	0.07 0.17 2	0.14 0.02 2
HIP 87629	-0.03 0.06 6	0.04 0.04 4	0.03 0.03 5	0.03 0.06 6	-0.04 0.04 3	-0.05 0.05 4	0.02 0.04 11	0.02 0.15 2	0.22 0.02 2
HIP 94576	0.04 0.10 5	-0.01 0.02 4	0.08 0.05 5	0.08 0.05 6	0.04 0.04 3	0.04 0.05 4	0.08 0.05 11	0.13 0.25 2	0.13 0.01 2
HIP 95375	-0.06 0.07 6	-0.02 0.05 4	-0.01 0.02 5	0.01 0.04 6	-0.01 0.02 3	0.00 0.05 4	0.07 0.06 11	0.17 0.27 2	0.11 0.02 2
HIP 96028	-0.03 0.06 6	0.02 0.04 4	-0.02 0.03 5	-0.03 0.05 6	-0.12 0.07 3	0.01 0.06 4	0.04 0.05 11	0.07 0.19 2	0.11 0.04 2
HIP 96294	-0.02 0.07 6	0.06 0.05 4	0.04 0.03 5	0.02 0.05 6	-0.06 0.06 3	0.03 0.07 4	0.06 0.04 11	0.08 0.20 2	0.17 0.04 2
HIP 102010	0.01 0.01 5	0.09 0.03 4	0.05 0.06 5	-0.02 0.05 6	-0.11 0.05 3	0.07 0.03 4	0.06 0.05 10	0.18 0.29 2	0.05 0.04 2
HIP 104035	-0.01 0.07 6	0.06 0.04 4	0.01 0.03 5	0.01 0.04 6	-0.10 0.03 3	-0.06 0.06 4	-0.01 0.05 11	-0.08 0.08 2	0.31 0.03 2
HIP 105502	-0.08 0.07 5	0.06 0.01 4	-0.06 0.05 5	-0.04 0.05 6	-0.15 0.04 3	-0.05 0.05 4	0.02 0.07 11	0.04 0.16 2	0.13 0.08 2
HIP 106551	-0.08 0.07 5	-0.01 0.05 4	0.03 0.05 5	-0.05 0.07 6	-0.10 0.04 3	-0.02 0.05 4	0.03 0.06 11	0.14 0.30 2	0.08 0.02 2
HIP 107502	0.01 0.08 7	-0.01 0.02 4	0.02 0.06 5	-0.01 0.03 6	-0.02 0.05 3	0.01 0.06 4	0.06 0.06 11	0.09 0.21 2	0.18 0.01 2
HIP 108012	0.01 0.07 7	-0.08 0.06 4	-0.01 0.02 5	-0.01 0.04 6	-0.02 0.05 3	0.03 0.07 4	0.06 0.07 11	0.11 0.31 2	0.20 0.10 2
HIP 108914	-0.06 0.09 5	-0.02 0.05 4	0.01 0.06 5	0.01 0.05 6	-0.04 0.02 3	0.05 0.06 4	0.10 0.05 11	0.11 0.25 2	0.07 0.06 2
HIP 109387	0.00 0.06 6	0.02 0.03 4	0.01 0.06 5	0.00 0.06 6	-0.07 0.02 3	-0.05 0.04 4	0.03 0.06 11	0.06 0.12 2	0.15 0.07 2
HIP 109585	-0.01 0.08 6	0.01 0.03 4	0.06 0.04 5	0.00 0.04 6	-0.02 0.05 3	0.06 0.08 4	0.07 0.04 11	0.17 0.29 2	0.13 0.06 2
HIP 111728	0.06 0.06 7	-0.10 0.05 4	0.09 0.06 5	0.04 0.07 6	-0.01 0.06 3	0.11 0.07 4	0.16 0.06 11	0.19 0.37 2	-0.01 0.01 2
HIP 113144	0.04 0.07 6	0.11 0.02 4	0.05 0.04 5	-0.02 0.06 6	-0.05 0.05 3	0.02 0.08 4	0.04 0.03 11	0.04 0.04 2	0.22 0.17 2
HIP 114742	-0.03 0.05 8	-0.03 0.02 4	0.01 0.05 5	0.02 0.06 6	-0.11 0.09 3	0.11 0.08 4	0.10 0.07 11	0.18 0.40 2	0.08 0.05 2
HIP 115899	-0.02 0.07 6	0.09 0.05 4	-0.02 0.02 5	-0.03 0.05 6	-0.06 0.05 3	-0.02 0.05 4	0.01 0.05 11	0.02 0.08 2	0.33 0.07 2
HIP 116348	0.00 0.06 8	0.02 0.01 3	-0.01 0.05 5	-0.01 0.06 6	-0.07 0.02 3	0.02 0.05 4	0.04 0.05 11	0.00 0.11 2	0.20 0.04 2
HIP 116644	-0.07 0.05 6	0.04 0.03 4	-0.04 0.04 5	-0.03 0.05 6	-0.13 0.05 3	-0.04 0.04 4	0.01 0.05 11	0.05 0.13 2	0.23 0.04 2

Table 7. Abundance sensitivities to various parameters for the star HIP 8926

Quantity	N	$\sigma(T_{\text{eff}})$	$\sigma(\log g)$	$\sigma(\xi_t)$	$\sigma([M/H])$	$\overline{\sigma}(W_\lambda)$	σ_{model}
[Na I/Fe]	2	± 0.04	± 0.01	± 0.06	± 0.01	± 0.02	± 0.08
[Mg I/Fe]	4	± 0.03	± 0.01	± 0.05	± 0.00	± 0.02	± 0.06
[Al I/Fe]	4	± 0.04	± 0.01	± 0.03	± 0.01	± 0.02	± 0.06
[Si I/Fe]	5	± 0.03	± 0.06	± 0.05	± 0.02	± 0.02	± 0.09
[Ca I/Fe]	8	± 0.05	± 0.02	± 0.10	± 0.01	± 0.01	± 0.11
[Sc II/Fe]	6	± 0.01	± 0.10	± 0.03	± 0.04	± 0.02	± 0.11
[Ti I/Fe]	8	± 0.07	± 0.01	± 0.05	± 0.01	± 0.01	± 0.09
[Ti II/Fe]	4	± 0.02	± 0.11	± 0.12	± 0.04	± 0.03	± 0.17
[V I/Fe]	5	± 0.08	± 0.01	± 0.04	± 0.01	± 0.02	± 0.10
[Cr I/Fe]	6	± 0.05	± 0.00	± 0.08	± 0.02	± 0.02	± 0.10
[Mn I/Fe]	3	± 0.05	± 0.01	± 0.05	± 0.01	± 0.02	± 0.07
[Fe I/H]	57	± 0.03	± 0.03	± 0.08	± 0.02	± 0.01	± 0.10
[Fe II/H]	8	± 0.06	± 0.13	± 0.09	± 0.04	± 0.02	± 0.17
[Co I/Fe]	4	± 0.03	± 0.03	± 0.04	± 0.02	± 0.02	± 0.06
[Ni I/Fe]	11	± 0.02	± 0.04	± 0.09	± 0.02	± 0.02	± 0.10
[Zn I/Fe]	2	± 0.04	± 0.07	± 0.10	± 0.03	± 0.04	± 0.14
[Ba II/Fe]	2	± 0.01	± 0.06	± 0.13	± 0.04	± 0.02	± 0.15

Table 8. Comparisons with Pakhomov et al. (2011) for common stars. Δ represents the difference (current value - Pakhomov et al.).

Quantity	HIP 105502	HIP 106551	HIP 107502	HIP 108012	HIP 109585	HIP 116348	HIP 32844	HIP 35146	HIP 9307	HIP 94576	HIP 96028	Mean $\pm\sigma$
$\Delta[\text{Na I/H}]$	0.13	0.04	0.19	-0.04	0.00	0.08	-0.11	0.08	0.06	0.19	0.07	0.06 ± 0.09
$\Delta[\text{Mg I/H}]$	0.10	0.00	0.07	0.05	0.07	0.01	-0.21	-0.04	-0.01	0.02	0.05	0.01 ± 0.08
$\Delta[\text{Al I/H}]$	0.04	0.06	0.21	-0.07	-0.01	0.11	-0.1	0.07	-0.04	0.06	-0.05	0.03 ± 0.09
$\Delta[\text{Si I/H}]$	0.04	0.03	-0.02	0.07	-0.11	0.00	-0.08	-0.16	-0.07	-0.19	0.08	-0.04 ± 0.09
$\Delta[\text{Ca I/H}]$	-0.03	0.03	-0.07	-0.32	-0.14	-0.23	-0.34	-0.17	-0.30	0.04	-0.08	-0.15 ± 0.14
$\Delta[\text{Sc II/H}]$	0.19	0.01	0.37	-0.06	-0.10	-0.03	-0.10	-0.01	0.01	0.08	-0.07	0.03 ± 0.14
$\Delta[\text{Ti I/H}]$	0.14	-0.02	0.37	0.01	-0.01	0.10	-0.18	-0.01	0.10	0.10	0.01	0.06 ± 0.14
$\Delta[\text{V I/H}]$	0.10	-0.11	0.26	-0.17	-0.02	0.04	-0.16	-0.04	0.12	0.17	-0.17	0.01 ± 0.15
$\Delta[\text{Cr I/H}]$	0.10	-0.04	0.20	-0.06	-0.09	0.01	-0.07	-0.06	0.00	0.06	-0.03	0.01 ± 0.09
$\Delta[\text{Mn I/H}]$	0.24	0.16	0.34	0.14	0.15	0.00	-0.01	0.22	0.11	0.36	0.09	0.16 ± 0.12
$\Delta[\text{Fe I/H}]$	0.14	0.02	0.19	-0.01	-0.07	0.01	-0.08	0.03	0.01	0.05	0.04	0.03 ± 0.08
$\Delta[\text{Fe II/H}]$	0.17	0.04	0.21	-0.01	-0.07	0.06	-0.07	0.05	0.05	0.06	0.03	0.05 ± 0.09
$\Delta[\text{Co I/H}]$	0.07	0.02	0.26	-0.02	0.07	0.08	-0.06	0.01	0.05	0.18	0.04	0.06 ± 0.09
$\Delta[\text{Ni I/H}]$	0.19	0.07	0.26	0.04	-0.03	0.06	-0.09	0.07	0.05	0.07	0.06	0.07 ± 0.09
$\Delta[\text{Ba II/H}]$	0.34	0.06	0.55	0.11	0.02	0.50	0.26	0.23	0.26	0.24	0.14	0.25 ± 0.17
$\Delta T_{\text{eff}}(\text{K})$	160	50	290	20	80	140	-23	115	168	250	20	115 ± 98
$\Delta \log g$ (cgs)	0.66	0.13	1.10	0.18	0.00	0.32	0.05	0.34	0.48	0.50	0.08	0.35 ± 0.33
$\Delta \xi_t$ (km s $^{-1}$)	0.14	0.3	0.01	0.14	0.18	0.14	0.15	0.00	0.06	0.14	0.03	0.12 ± 0.08

Table 9. El/Fe for three [Fe/H] intervals : [Fe/H] = -0.2 to 0.0, 0.0 to +0.20 and +0.20 to +0.40 for our sample of Hercules stream giants and the local giants of Luck & Heiter (2007)

Entity	[Fe/H] interval = -0.2 to 0.0		[Fe/H] interval = 0.0 to +0.20		[Fe/H] interval = +0.20 to +0.40	
	Luck & Heiter 2007	Hercules stream	Luck & Heiter 2007	Hercules stream	Luck & Heiter 2007	Hercules stream
	Mean σ N	Mean σ N	Mean σ N	Mean σ N	Mean σ N	Mean σ N
[Na/Fe]	0.10 0.07 114	0.07 0.05 8	0.13 0.07 131	0.09 0.06 30	0.23 0.07 14	0.24 0.11 18
[Mg/Fe]	0.09 0.13 95	0.06 0.04 8	0.09 0.10 115	0.03 0.06 30	0.14 0.10 13	0.00 0.06 18
[Al/Fe]	0.10 0.08 113	0.16 0.05 8	0.08 0.05 129	0.11 0.07 30	0.13 0.07 14	0.13 0.06 18
[Si/Fe]	0.12 0.05 116	0.08 0.03 8	0.13 0.06 133	0.07 0.03 30	0.18 0.06 14	0.06 0.04 18
[Ca/Fe]	-0.03 0.07 116	0.07 0.03 8	-0.07 0.07 133	0.02 0.04 30	-0.17 0.06 14	-0.03 0.05 18
[Sc/Fe]	-0.07 0.07 116	0.02 0.06 8	-0.13 0.08 133	0.02 0.03 30	-0.16 0.10 14	0.12 0.43 18
[Ti/Fe]	-0.00 0.03 113	0.06 0.03 8	-0.01 0.03 132	0.01 0.04 30	-0.02 0.04 14	-0.03 0.04 18
[V/Fe]	-0.08 0.08 113	0.06 0.03 8	-0.04 0.08 128	0.01 0.04 30	0.06 0.10 14	0.01 0.06 18
[Cr/Fe]	0.02 0.09 114	0.01 0.03 8	0.03 0.04 133	-0.01 0.03 30	0.06 0.04 14	0.01 0.04 18
[Mn/Fe]	0.07 0.07 114	-0.09 0.02 8	0.17 0.12 131	-0.07 0.04 30	0.30 0.12 14	-0.05 0.04 18
[Co/Fe]	0.07 0.08 113	0.01 0.03 8	0.10 0.09 130	0.01 0.04 30	0.19 0.09 14	0.03 0.06 18
[Ni/Fe]	0.00 0.04 116	0.03 0.01 8	0.03 0.04 130	0.04 0.02 30	0.08 0.03 14	0.08 0.04 18
[Zn/Fe]	-0.04 0.29 3	0.05 0.07 8	0.04 0.07 3	0.08 0.07 30	— — —	0.11 0.07 18
[Ba/Fe]	0.03 0.18 114	0.22 0.07 8	-0.10 0.18 133	0.24 0.08 30	-0.37 0.17 14	0.14 0.10 18

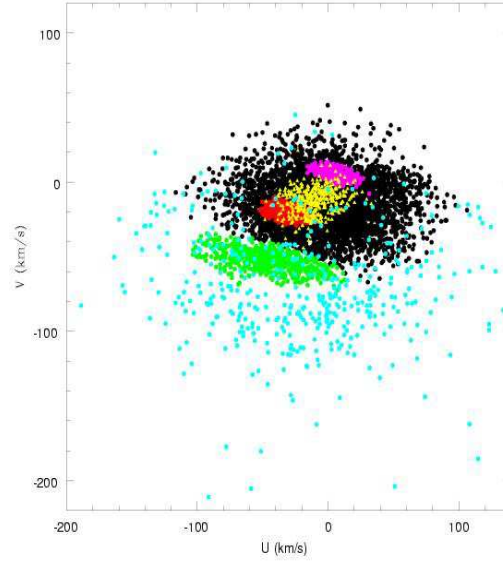


Figure 1. *Hipparcos* giants plotted in the U, V -plane. Six different groups are represented. The Hercules stream is represented by the green circles. The Hyades-Pleiades supercluster and the Sirius moving group are represented by red and magenta circles, respectively. Three groups of field stars are shown: young giants by yellow circles, high-velocity giants by blue circles and a smooth background of low-velocity stars by black circles. See Famaey et al. (2005) for detailed descriptions of these six groups. Credit: B. Famaey et al., A&A, 430, 165, 2005, reproduced with permission © ESO

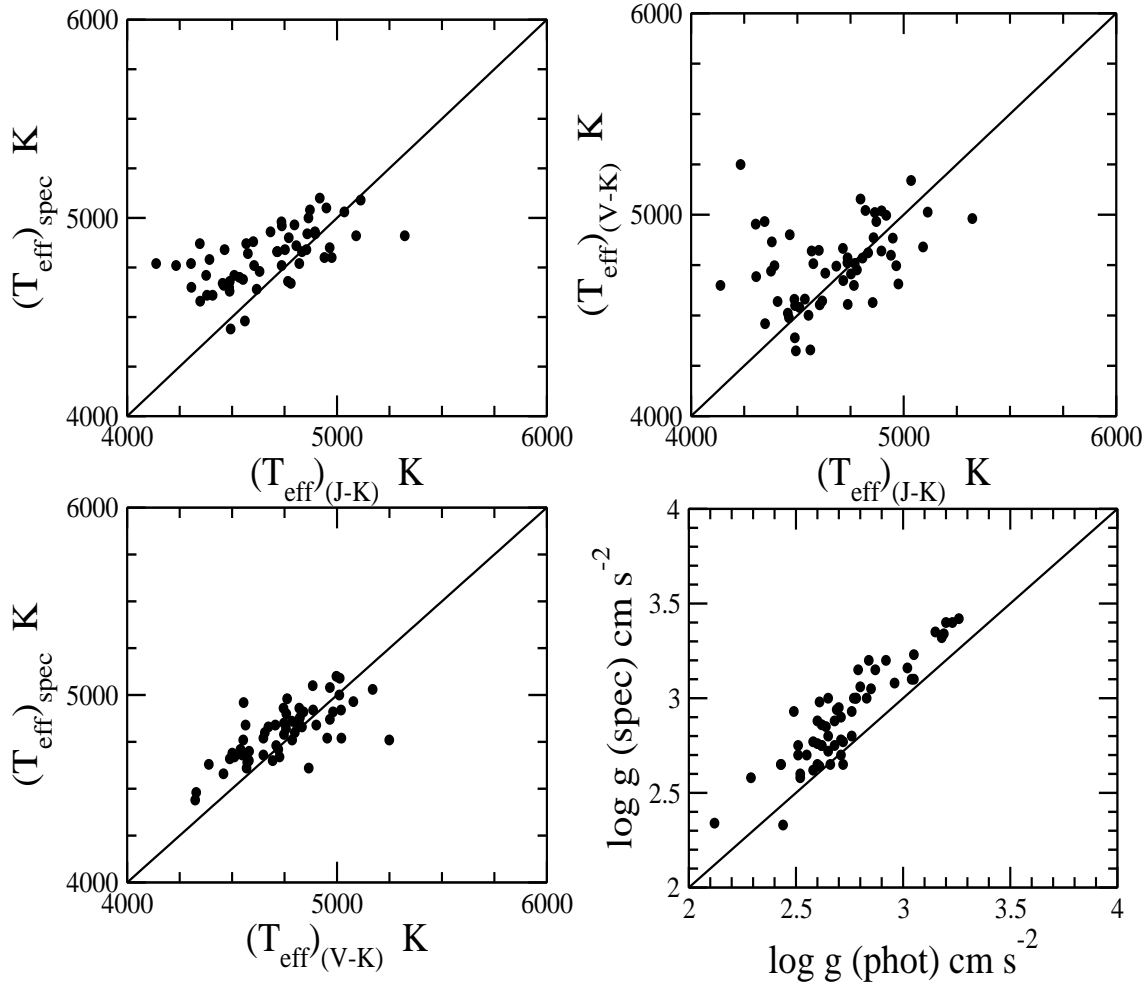


Figure 2. Comparison of photometric and spectroscopic atmospheric parameters. The top two panels compare the effective temperatures from spectroscopy $(T_{\text{eff}})_{\text{spec}}$ with the photometric temperature from either $(J - K)$ or $(V - K)$. The third panel from the top compares the photometric temperatures from $(V - K)$ and $(J - K)$. The bottom panel compares the spectroscopic $\log g$ with that derived from photometry. In all panels, the solid line has unit slope, i.e., $x=y$.

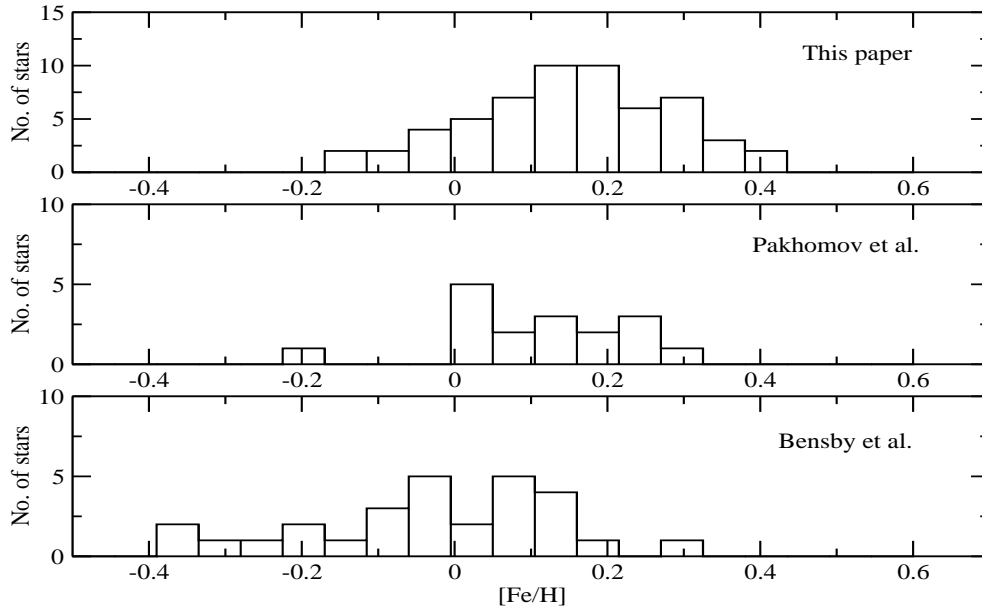


Figure 3. Histograms of the Iron abundance $[\text{Fe}/\text{H}]$ for samples of stars attributed to the Hercules stream. Top panel shows $[\text{Fe}/\text{H}]$ for our sample of 58 giants. The middle panel shows $[\text{Fe}/\text{H}]$ from the 17 giants analysed by Pakhomov et al. (2011). The bottom panel shows $[\text{Fe}/\text{H}]$ from the sample of dwarfs analysed by Bensby et al. (2014) and attributed in Section 4 to the Hercules stream.

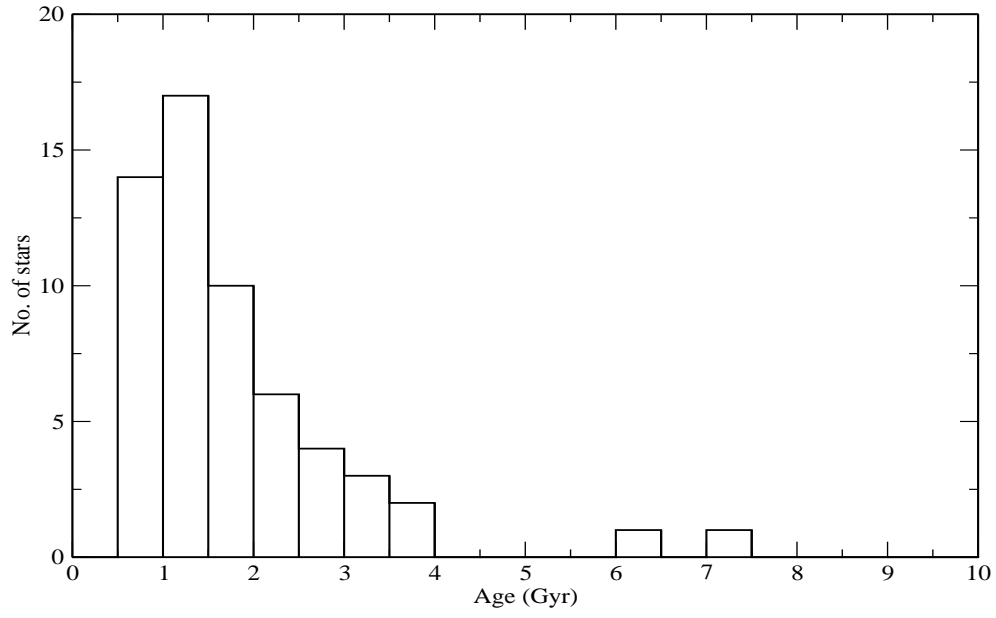


Figure 4. The age distribution of the 58 giant members of the Hercules stream. Bin size = 0.5 Gyr

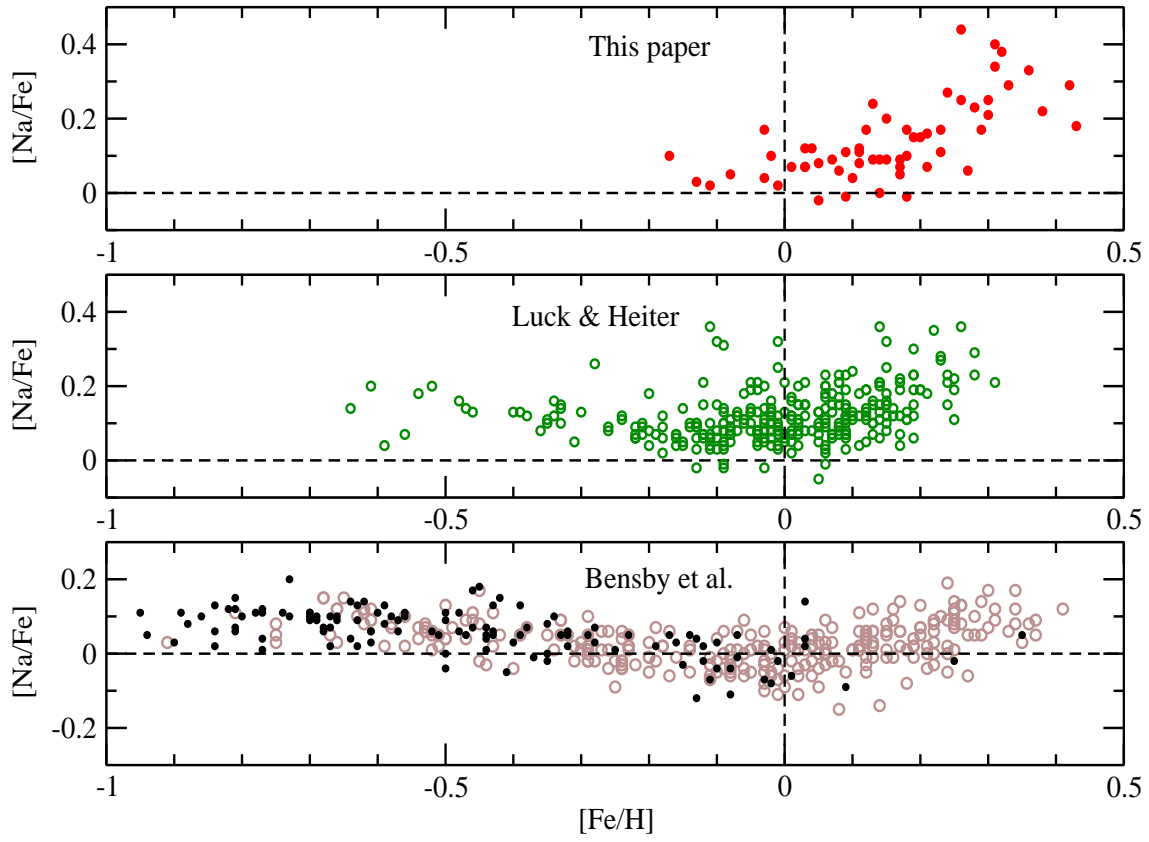


Figure 5. $[\text{Na}/\text{Fe}]$ versus $[\text{Fe}/\text{H}]$ for our Hercules giants (top panel), local giants analysed by Luck & Heiter (2007) (middle panel) and thin disc dwarfs (brown unfilled circles) and thick disc dwarfs (filled black circles) from Bensby et al. (2014).

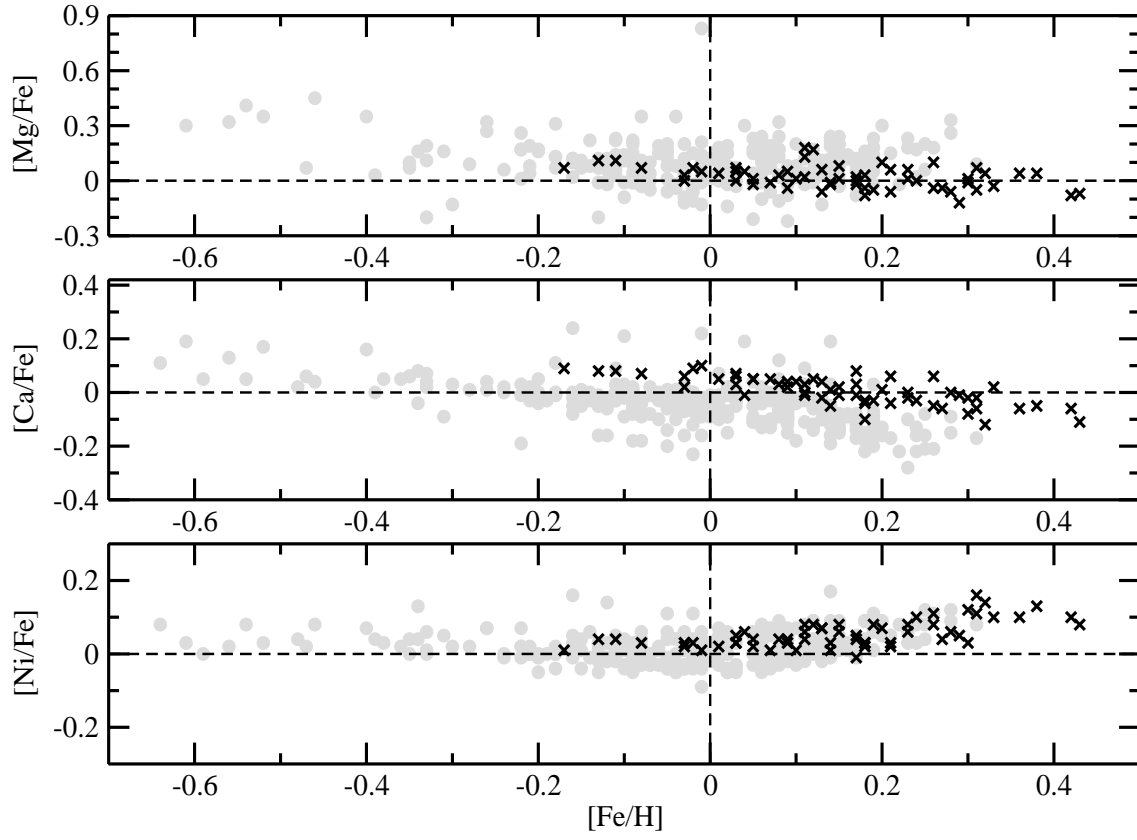


Figure 6. $[El/Fe]$ versus $[Fe/H]$ for $El = Mg, Si$ and Ni . In each panel, data for two samples are plotted: the Hercules stream giants (black crosses) and local giants (grey filled circles) from Luck & Heiter (2007).

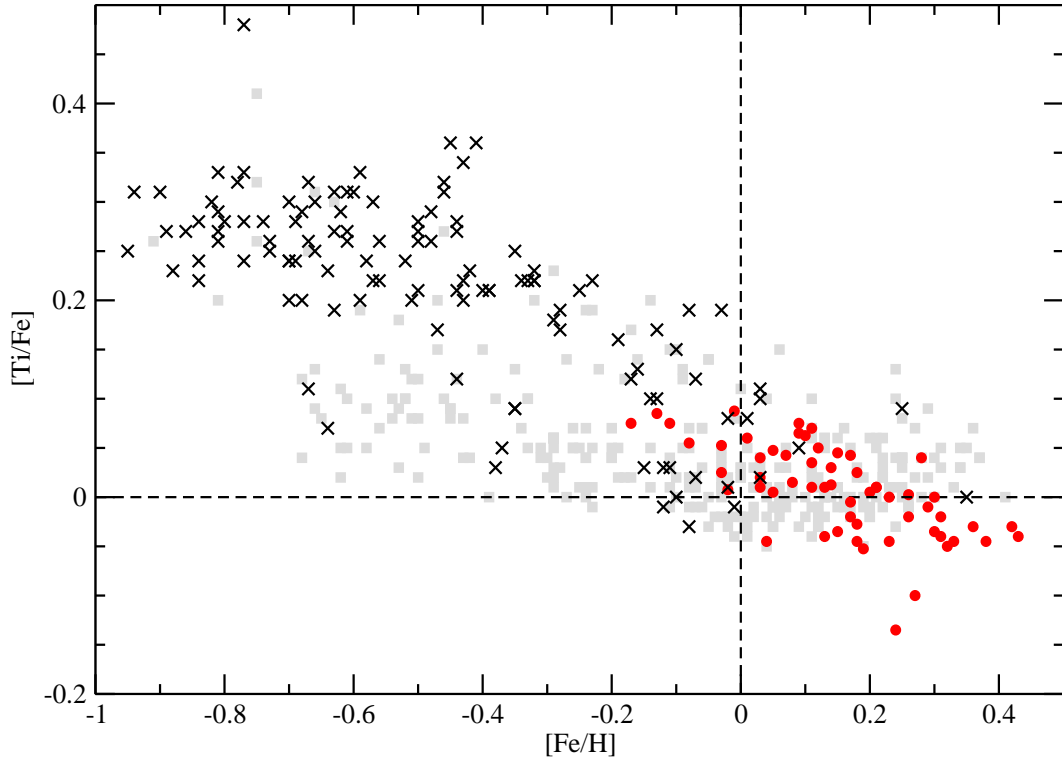


Figure 7. $[Ti/Fe]$ versus $[Fe/H]$ for thin disc, thick disc and Hercules stream stars. Hercules stream giants are represented by red filled circles. Thin and thick disc dwarfs are taken from Bensby et al. (2014). Thin disc dwarfs with a ratio of thin to thick disc membership probability greater than 10 are represented by grey squares and thick disc dwarfs with a ratio of thick to thin disc membership probability of greater than 10 are represented by the black crosses.